REPORT DOCUMENTATION PAGE

Form Approved
OMB No. 0704-0188

1. AGENCY USE ONLY (Leave blank)	2. REPORT DATE	3. REPORT TYPE AND DATES COVERED
	21 Sept. 95	Final Report, 4/15/94 - 4/14/95

4. TITLE AND SUBTITLE
Synthesis of High-Temperature, Monolithic Ceramic Bodies and Composites by the Oxidation of Solid, Metal-Bearing Precursors

5. FUNDING NUMBERS
G: F49620-94-1-0225

6. AUTHOR(S)
Ken H. Sandhage, Hamish L. Fraser

AFOSR-TR-97
0353

7. PERFORMING ORGANIZATION NAME(S) AND ADDRESS(ES)
The Ohio State University
Department of Materials Science & Engineering
Columbus, OH

9. SPONSORING/MONITORING AGENCY NAME(S) AND ADDRESS(ES)
Air Force Office of Scientific Research
110 Duncan AVe, Suite B 115
Bolling AFB, DC 20332-8050

NL

10. SPONSORING/MONITORING AGENCY REPORT NUMBER
F49620-94-1-0225

11. SUPPLEMENTARY NOTES

12a. DISTRIBUTION/AVAILABILITY STATEMENT
Approved for public release; distribution unlimited.

12b. DISTRIBUTION CODE

13. ABSTRACT (*Maximum 200 words*)

This one-year project has been focused on synthesizing near net-shaped celsian and celsian composites by the oxidation of solid, alkaline-earth-metal-bearing precursors. Key results are:

- Near net-shaped bodies of celsian and celsian-zirconia composites were produced from Ba(Sr)-Al-Al_2O_3-SiO_2 and Ba-Al_2O_3-Si-SiO_2-ZrO_2 precursors, respectively. Monoclinic celsian and celsian-zirconia composites were synthesized at ≥1200°C. Altex™ fiber-bearing composites were also produced at ≥1260°C.
- The reaction path to celsian from Ba-Al-Si precursors was evaluated. Barium oxidized rapidly at 300°C. The resulting BaO_2 reacted with Si at 300-500°C to yield Ba_2SiO_4. Appreciable Al oxidation occurred during heating from 500 to 800°C. Continued oxidation of Si and reaction of SiO_2 with Al_2O_3 and Ba_2SiO_4 at 800-1100°C led to other intermediate silicates and then to hexacelsian. Monoclinic celsian formed at 1200-1260°C.
- With Ba-Al-Al_2O_3-SiO_2 precursors, extensive Ba_2SiO_4 formation also occurred at 300°C. However, $BaAl_2O_4$ was produced at 300-650°C. Between 650 and 900°C, hexacelsian formation commenced at the expense of barium aluminate, silica, and barium silicates. Appreciable hexacelsian formation was observed after 35 hours at 1200°C. Monoclinic celsian formed from hexacelsian at ≥1200°C. Partial Sr or Mg substitution for Ba enhanced the formation of monoclinic celsian. Mg substitution also led to the formation of barium osumilite.

14. SUBJECT TERMS	15. NUMBER OF PAGES
Net Shape, Celsian, Ceramic Composites, Oxidation, Metal-Bearing Precursors, Phase Evolution	49
	16. PRICE CODE

17. SECURITY CLASSIFICATION OF REPORT	18. SECURITY CLASSIFICATION OF THIS PAGE	19. SECURITY CLASSIFICATION OF ABSTRACT	20. LIMITATION OF ABSTRACT
UNCLASSIFIED	UNCLASSIFIED	UNCLASSIFIED	UL

Final Project Report

Synthesis of High-Temperature, Monolithic Ceramic Bodies and Ceramic-Matrix Composites by the Oxidation of Solid Metal-Bearing Precursors (SMP)

AFOSR Grant #F49620-94-1-0225

Project Duration: April 15, 1994 - April 14, 1995

Principal Investigators:

Prof. Ken H. Sandhage
Department of Materials Science & Engineering
The Ohio State University
Columbus, OH
(614) 292-6731
Fax: (614) 292-1537

Prof. Hamish L. Fraser
Ohio Regents Eminent Scholar
Department of Materials Science & Engineering
The Ohio State University
Columbus, OH
(614) 292-2708
Fax: (614) 292-1537

Ohio State University Program Officer

Arthur S. Rundle
Sponsored Program Officer
Research Foundation
The Ohio State University
(614) 292-1673
Fax: (614) 292-4315

I. Executive Summary

This one-year project has been focused on an exciting new (patented) method for preparing alkaline-earth-bearing ceramics and composites for high-temperature structural applications: the oxidation of solid metal-bearing precursors (SMP). This novel process consists of two basic steps: (i) preparation of solid metal-bearing precursors of desired composition, microstructure, and shape, and (ii) oxidation to yield monolithic ceramics or ceramic composites that *retain the precursor shape.* The key to the SMP process is to start with malleable precursors containing alkaline earth (AE) and non-alkaline earth metals. AE metals and alloys oxidize rapidly at modest temperatures. Further, the molar volumes of most AE metals are greater than the molar volumes of corresponding oxides (e.g., $V_m(Ba) > V_m(BaO_2)$). The opposite is true for non-AE elements. As a result, the net volume change incurred from oxidation of an intimate mixture (or alloy) of AE and non-AE metals can be relatively small. This volume change can be further reduced (in principal to zero) by replacing an appropriate fraction of metal phases with oxides. Hence, the SMP method offers the potential for net-shape processing of AE-bearing ceramics and composites. An attractive AE-bearing ceramic for high-temperature composites is celsian, $BaAl_2Si_2O_8$. Celsian has a high melting point (1760°C), good thermal shock resistance, a low density (3.39 g/cm^3), excellent oxidation resistance, and chemical compatibility with such reinforcements as alumina, mullite, or zirconia. Building upon preliminary studies at OSU, work over the past year has been focused on synthesizing celsian and celsian-based composites.

The specific goals of this one-year project have been to: 1) develop better understanding of phase/microstructural evolution during the transformation of metallic and metal-oxide precursors into celsian, 2) demonstrate the fabrication of near net-shaped celsian bodies, and 3) evaluate the syntheses of celsian composites. Key results of fundamental or engineering nature are:

- The reaction path to celsian from Ba-Al-Si precursors over the temperature range of 300-1260°C has been evaluated using XRD, SEM/EDX, EPMA/WDX, and TEM analyses:
  - Barium oxidized rapidly at 300°C. The resulting BaO_2 reacted primarily with Si at 300-500°C to yield Ba_2SiO_4. High-resolution TEM revealed that this reaction involved the formation of a thin layer of amorphous silicate located between BaO_2 and Ba_2SiO_4.
  - Al particles in the precursor were completely oxidized during heating from 500 to 800°C. Continued oxidation of Si and reaction of resulting SiO_2 with Al_2O_3 and with Ba_2SiO_4 at 800-1100°C led to the formation of other intermediate silicates and then hexacelsian.
  - Monoclinic celsian formed from hexacelsian at 1200-1260°C in less time than has been reported for other precursors. TEM analyses revealed the presence of an amorphous silicate that should have been a liquid at 1200°C. Such liquid may have enhanced the hexacelsian-to-monoclinic transformation (via a dissolution/reprecipitation mechanism).
- The formation of celsian from Ba-Al-Al_2O_3-SiO_2 precursors has also been evaluated:
  - Extensive Ba_2SiO_4 formation again occurred at 300°C. Unlike for Ba-Al-Si precursors, however, $BaAl_2O_4$ was produced at 300-650°C. The presence of Al_2O_3 in the precursor appears to have allowed for the formation of $BaAl_2O_4$ prior to complete consumption of BaO_2 by the concurrent reaction of BaO_2 with SiO_2 (to form Ba_2SiO_4).
  - As for Ba-Al-Si, hexacelsian preceded the formation of monoclinic celsian. However, partial substitution of Sr or Mg for Ba in these precursors dramatically enhanced the rate of formation of monoclinic celsian at ≤1200°C. Partial substitution of Mg for Ba also led to the formation of an appreciable amount of barium osumilite, $BaMg_2Al_6Si_9O_{30}$.
- Composites consisting of only monoclinic celsian and zirconia were produced after firing for 26 hours at 1200°C. XRD analyses indicated that appreciable solid solubility of zirconia in celsian is possible at 1200°C. Composites of $BaAl_2Si_2O_8$ with Al_2O_3-rich fibers were also produced. Appreciable chemical reaction with the fibers at ≤1260°C was not observed.
- Near net-shaped pellets of monoclinic celsian and celsian-zirconia composites have been produced upon complete transformation of Ba-Al-Al_2O_3-SiO_2, Ba-Sr-Al-Al_2O_3-SiO_2, and Ba-Al_2O_3-Si-SiO_2-ZrO_2 precursors. Dimensional changes of ≤1% were achieved.

Table of Contents

Pages

II. Introduction

The requirements of stiffness, toughness, light weight, and high-temperature strength make fiber-reinforced, ceramic-matrix composites potentially attractive for advanced engine components in the transportation (aircraft, diesel trucks), defense, and electric utility industries. However, in order to realize such potential, improved processing methods capable of producing dense, complex-shape, refractory-matrix composites at modest cost are needed.

A novel method for synthesizing alkaline-earth-bearing ceramics is the oxidation of solid metal-bearing precursors (SMP) [1-18]. Work over the past few years at Ohio State University has demonstrated that dense, shaped dielectric ($BaTiO_3$), ferrimagnetic ($BaFe_{12}O_{19}$), and proton-conducting ($Ba(Ce,Nd)O_3$) ceramics can be produced at modest temperatures by the oxidation of metallic or metal/oxide precursors [1-7]. A number of authors, including one of the PIs, have also produced superconducting oxide composites from all-metallic precursors [8-15]. A unique and key feature of the work at OSU has been the recognition that alkaline earth and non-alkaline earth metals exhibit opposite volume changes upon oxidation, which has led to the concept of tailoring the precursor phase content so as to produce near net-shaped ceramic bodies upon oxidation [16, 17].

Preliminary work (conducted just prior to this present AFOSR program) at OSU indicated that the SMP method could also be used to produce the high-temperature silicate compound known as celsian, $BaAl_2Si_2O_8$ [18]. Celsian is an attractive matrix phase for ceramic composites, owing to its high melting temperature (1760°C), excellent high-temperature oxidation resistance (unlike SiC), relatively good thermal shock resistance (owing to an average linear thermal expansion coefficient of only $2.3X10^{-6}$/°C from 20° to 1000°C), and modest density (3.39 g/cm^3) [19, 20]. Celsian is also chemically compatible with Al_2O_3, $Al_6Si_2O_{13}$ (mullite), ZrO_2, and Si_3N_4 reinforcements (i.e., fibers, particles) [21-28]. While this early work had revealed that shaped monolithic celsian could be produced by the SMP method, a detailed fundamental understanding of the transformation mechanisms (reaction paths, microstructural evolution) and the effects of SMP processing conditions (e.g., precursor phase content, doping effects, etc.) on such transformations were not known. The syntheses of celsian-based composites was also not thoroughly examined. Before discussing the results of work conducted over the past year in this AFOSR-sponsored program, a general description of the SMP method, and its advantages relative to other processing routes, will be presented.

A. General Description of the SMP Method

This novel process consists of two basic steps:

1) Precursor Preparation - A multicomponent, alkaline-earth-metal-bearing precursor with an appropriate composition, phase content, and shape is prepared. The composition of the precursor (i.e., the relative amount of each element, whether that element is present in one or more oxide or metallic phases) is determined by the phase(s) desired upon complete transformation. The phase content (i.e., the relative amounts and types of metal, intermetallic, or oxide phases) is chosen so as to minimize the net volume change upon transformation.

2) Oxidation/Annealing - The solid, metal-bearing precursor body is oxidized and then further annealed to produce a dense, near net-shaped multicomponent ceramic or ceramic-matrix composite.

General schemata of SMP methods for producing shaped, bulk monolithic ceramics are illustrated in Figure 1 on the following page.

II. Introduction (cont.)

A. General Description of the SMP Method (cont.)

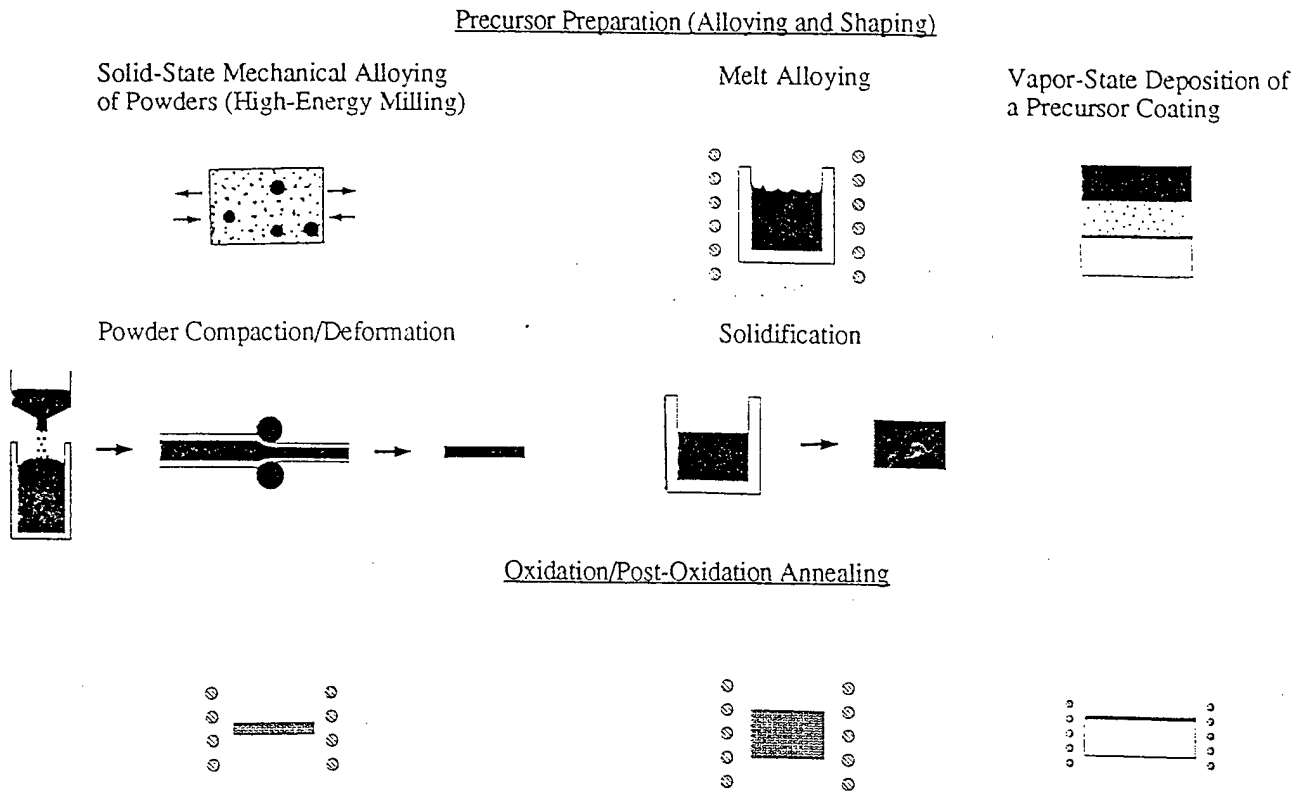

Figure 1. Solid metal-bearing precursor (SMP) routes to bulk, monolithic ceramic components.

The key to the SMP method is the use of alkaline-earth-metal-bearing precursors. As discussed in more detail in the following sections, such precursors can be readily formed into desired shapes, can be oxidized at a rapid, but controllable rate, and can be transformed at modest temperatures into dense, near net-shaped ceramic bodies.

Before proceeding further, it is important to note that the SMP method is distinctly different from other oxidation processes, such as self-propagating high-temperature synthesis (SHS) [29, 30], reaction-bonded aluminum oxide (RBAO) [31-34], directed metal oxidation (DIMOX) [35-37], or the co-continuous ceramic composite (C^4) process [38-40]. While exothermic, self-sustaining combustion reactions allow for SHS processing of a wide variety of carbides, nitrides, oxides, and silicides with modest energy input, the resulting ceramic bodies are often relatively porous [30] and tend not to retain the dimensions of the starting precursor. On the contrary, the RBAO, DIMOX, and C^4 processes are each capable of yielding near net-shaped, ceramic-bearing bodies. Accurate control of the dimensions of RBAO-derived bodies requires the presence of a specific amount of porosity within the starting precursor (in order to compensate for the volume expansion associated with the oxidation of aluminum). Such porosity is not required with the SMP process (i.e., it is possible to produce dense, near net-shaped ceramics from dense SMP bodies). The DIMOX process yields a ceramic-metal composite with a shape that is determined by the shape of the crucible (often ceramic) used to contain the molten metal during reaction with gaseous oxygen [35-37]. The C^4 process also yields ceramic-metal composites, although in this case the composites are produced by a displacement reaction between a molten metal (e.g., molten aluminum) and a solid oxide preform (e.g., silica glass). The shape of a C^4-derived composite is determined by the shape of the oxide preform [38-40]. The SMP method, however,

is capable of yielding near net-shaped, all-ceramic bodies without relying upon the use of a shaped ceramic crucible or a glass preform. Instead, the SMP route relies upon conventional metallurgical processing (e.g., mechanical alloying to produce a powder mixture or alloy which is compacted and formed by deformation processing) to yield shaped solid precursors that can then be transformed by oxidation into near net-shaped ceramics.

1. Precursor Preparation

A solid-state, powder metallurgical route can be a particularly effective method for producing shaped precursor bodies. Solid-state milling equipment (e.g., vibratory ball mills, attritor mills, rod mills) can be used to produce reactive precursor powders that, in turn, can be compacted and formed into desired shapes by standard deformation processes (e.g., pressing, rolling, extrusion, etc.). High-energy mechanical alloying has been demonstrated to be an effective method of fabricating metal-bearing precursors consisting of finely-divided, intimate mixtures of highly-reactive phases [5, 6, 9, 12, 16]. On the other hand, prolonged mechanical alloying can result in the extensive formation of brittle intermetallic compounds that may be difficult to form into complex shapes by room-temperature deformation processing [12]. The synthesis of highly-reactive, yet malleable alkaline-earth-bearing precursors requires careful control of milling parameters (milling temperature, time, rate) [1, 2, 6, 7, 12, 15, 16, 18].

The fabrication of a shaped precursor can also be conducted by melt casting (or so-called "compocasting," if a partially-molten metallic or metal+oxide precursor is cast). Planar flow casting (melt spinning) can be used to produce a precursor tape consisting of a finely-divided mixture of metallic and intermetallic phases [8, 10, 13]. A metallic precursor coating may also be produced by dipping a substrate into a molten alloy [14]. An example of a precursor system that may be suitable for melt casting is the Ba-Al-Si system. As shown in Figure 2 below, a melt with a $BaAl_2Si_2$ composition can be produced at 1040°C. This melt can be cast into a shaped

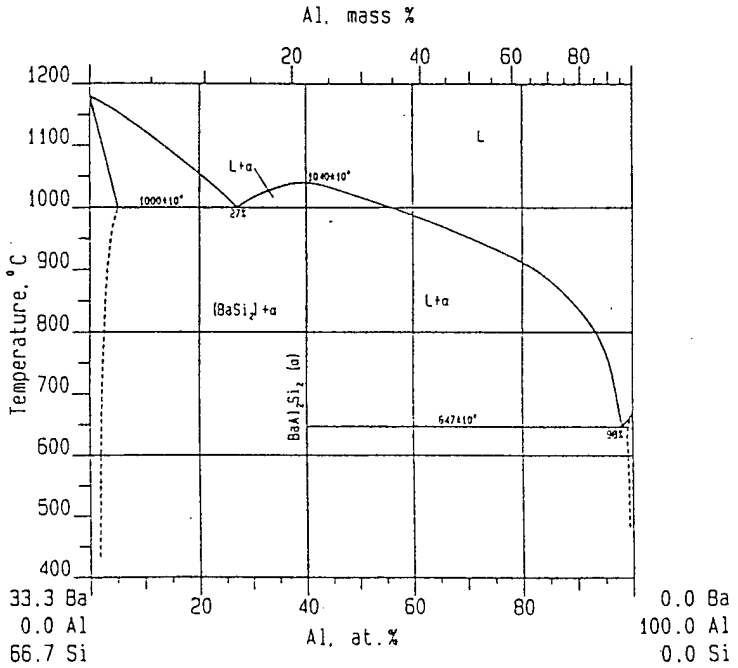

Fig. 2. The $BaSi_2$-Al phase diagram illustrating congruent melting of $BaAl_2Si_2$ at 1040°C [41].

II. Introduction (cont.)

A. General Description of the SMP Method (cont.)

1. Precursor Preparation (cont.)

precursor body composed of a $BaAl_2Si_2$ ternary compound, which possesses the same Ba:Al:Si elemental ratio as celsian ($BaAl_2Si_2O_8$). Preliminary tests conducted at OSU have indicated that molten alkaline-earth-bearing liquids (e.g., Ba-Al-Si, Ba-Al, and Mg) can be infiltrated into porous alumina preforms without requiring the use of externally-applied pressure [42].

2. Oxidation Processing

In order to produce a bulk ceramic component from a shaped metal-bearing precursor, the precursor should oxidize at a relatively rapid (although controllable) rate, preferably at a modest temperature. Most alkaline earth metals (Ba, Sr, Ca, Mg) oxidize (and nitridize) at a rapid, linear rate at temperatures below 500°C [43-49]. Hence, it may be expected that precursors containing significant concentrations of alkaline earth metals would also oxidize (and nitridize) rapidly at modest temperatures, so that bulk forms of such precursors could be completely oxidized in reasonable times. Indeed, this has been observed for a variety of alkaline-earth-bearing precursors (e.g., Ba-Ti precursors to $BaTiO_3$ [1, 2, 4, 5], Ba-Nd-CeH_3 precursors to $Ba(Ce,Nd)O_3$ [7], Ba-Fe precursors to $BaFe_{12}O_{19}$ [6], and Y-Ba-Cu, Bi-Sr-Ca-Cu, and Ba-Pb-Bi precursors to $YBa_2Cu_3O_y$, $Bi_2Sr_2Ca_1Cu_2O_y$, and $BaPb_xBi_{1-x}O_y$, respectively [8-13]).

In order to retain the precursor shape, the net volume change upon complete transformation should be minimized. Owing to significant volume expansions, the complete oxidation of most metals and alloys results in severe spallation and cracking [43]. The molar volumes of several elements and oxides are listed in Table 1 below. An exceptional feature of most alkaline earth metals (Mg, Ca, Sr, Ba) is that the molar volume of the metal is larger than the molar volume of the corresponding oxide(s) (e.g., $V_m(Ba) > V_m(BaO)$, $V_m(BaO_2)$). The opposite is true for other metals (e.g., $2V_m(Al) < V_m(Al_2O_3)$). Hence, an appropriate amount of alkaline earth metal can be mixed with non-alkaline earth metals and/or oxides such that the resulting precursor possesses the same overall molar volume as the desired product multicomponent oxide [17]. Consequently, the volume and dimensional changes upon oxidation and complete transformation of the precursor into the desired ceramic compound can be quite small or zero.

Table 1. Molar volumes of metals and oxides (at room temperature).

Element	V_m(element) (cm^3/mole)	Oxide	V_m(oxide) (cm^3/mole)	$100 \cdot \Delta V_m/\alpha V_m$(element)[1]
Ni	6.60	NiO	11.2	+70%
Cu	7.12	Cu_2O	23.8	+67%
Fe	7.11	FeO	12.6	+77%
Ti	10.6	TiO_2 (rutile)	18.8	+77%
Zr	14.1	ZrO_2 (monoclinic)	20.9	+48%
Al	9.99	Al_2O_3 (corundum)	25.7	+29%
Si	12.1	SiO_2 (quartz)	22.7	+88%
Ba	39.1	BaO	26.8	-31%
Ba	39.1	BaO_2	34.1	-13%
Sr	33.7	SrO	22.0	-35%
Sr	33.7	SrO_2	26.2	-22%
Ca	26.0	CaO	16.6	-36%
Ca	26.0	CaO_2	24.7	-5%
Mg	14.0	MgO	11.3	-19%

[1] $\Delta V_m/\alpha V_m(\text{element}) = [V_m(\text{oxide}) - \alpha V_m(\text{element})]/\alpha V_m(\text{element})$. α is the number of moles of the element present in one mole of oxide. For example, α for TiO_2 is one, while α for Cu_2O is 2.

II. Introduction (cont.)

A. General Description of the SMP Method (cont.)

2. Oxidation Processing (cont.)

Consider the following net oxidation reaction to produce celsian from a precursor consisting of an intimate mixture of Ba, Al, Al_2O_3, and SiO_2 with a $Ba:Al:Al_2O_3:SiO_2$ molar ratio of 1.00:1.68:0.16:2.00.

$$1.00\ Ba + 1.68\ Al + 0.16\ \alpha\text{-}Al_2O_3 + 2.00\ SiO_2(\text{cristobalite}) \xrightarrow[+\ O_2(g)]{\text{heat}} BaAl_2Si_2O_8 \quad (1)$$

The calculated percentage change in volume for this reaction is less than 0.1% (i.e., $100{\cdot}\Delta V_m/V_m(\text{precursor}) < +0.1\%$). Hence, the transformation of such a dense, finely-divided Ba-Al-Al_2O_3-SiO_2 precursor into dense celsian should result in a celsian component that retains the precursor shape. Celsian precursors with other metal and oxide phases can also be tailored to yield such small volume changes. For example, celsian precursors containing mullite, $3Al_2O_3{\cdot}2SiO_2$, or intermetallic phases, such as $BaAl_2Si_2$, could be fabricated. The metal and oxide contents of precursors to other alkaline-earth-bearing ceramics (e.g., $SrAl_2Si_2O_8$, $BaMg_2Al_6Si_9O_{30}$ (osumilite), $Mg_2Al_4Si_5O_{10}$ (cordierite), etc.) could be tailored in a similar fashion to yield dense, near net-shape ceramic bodies [17].

3. Fabrication of Composites

The SMP process illustrated in Fig. 1 can be modified to allow for the syntheses of ceramic-matrix composites. Consider the synthesis of a bulk, discontinuous-fiber-reinforced, celsian-matrix composite by the process illustrated in Figure 3. Metal-bearing precursor powder can be produced by solid-state mechanical alloying (e.g., high-energy ball milling). The precursor powder can be blended with ceramic fibers, and then packed and sealed into a fugitive metal tube. The packed tube can be formed into a desired shape by deformation processing (e.g., example, a thick sheet could be produced by rolling). The fugitive metal sheath can then be removed and the precursor can be completely oxidized and annealed to yield a dense fiber-reinforced ceramic-matrix composite. A similar process could be used to produce a particulate-reinforced ceramic-matrix composite.

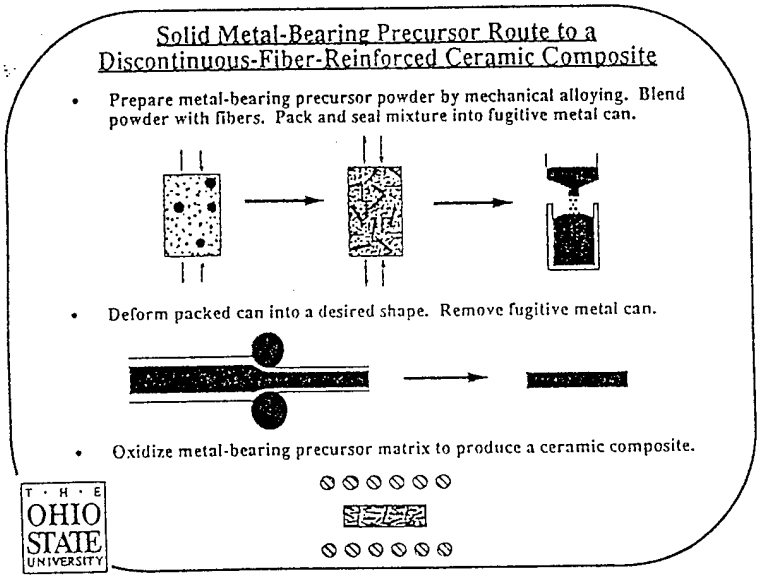

Figure 3. A solid metal-bearing precursor (SMP) route to ceramic-matrix composites [17]. A solid-state mechanical alloying/deformation approach is illustrated.

II. Introduction (cont.)

A. General Description of the SMP Method (cont.)

3. Fabrication of Composites (cont.)

Continuous-fiber-reinforced composites could be fabricated by the method illustrated in Figure 4. A molten metal precursor can be infiltrated into a fiber preform contained within a shaped mold. After solidification and mold removal, the solid precursor matrix can be completely oxidized and annealed to yield a dense, continuous-fiber-reinforced ceramic composite. For example, a molten $BaAl_2Si_2$ precursor could be infiltrated, solidified and then oxidized to produce a fiber-reinforced, celsian-matrix composite. Indeed, recent unpublished work at OSU has indicated that molten Ba-Al-Si, Ba-Al, and Mg can infiltrate into alumina preforms at ≤1200°C without the need for an externally applied pressure [42].

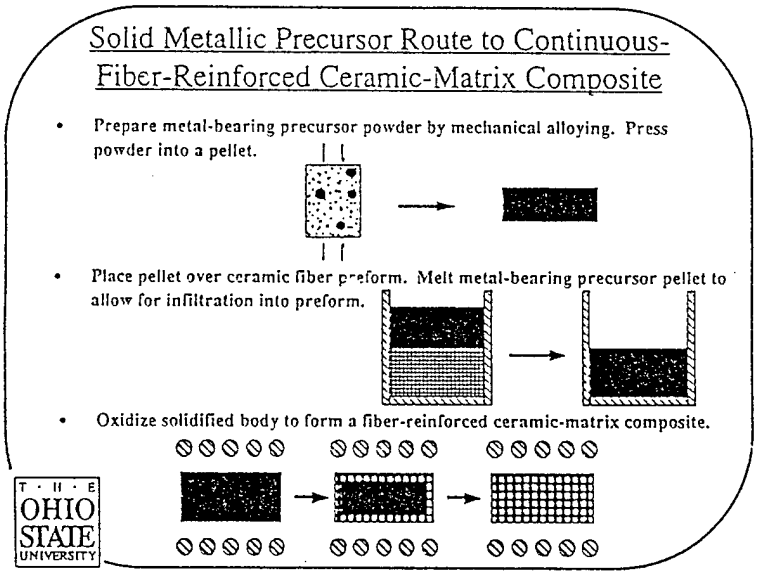

Fig. 4. A solid metal-bearing precursor (SMP) route to ceramic-matrix composites. A melt-infiltration/solidification approach for producing a precursor matrix is illustrated [17, 42].

B. Attractive Features of the SMP Method

The SMP process possesses a unique combination of advantages over other ceramic synthesis routes. Perhaps the most unique and important advantage is the ability to fabricate near net-shaped ceramic bodies by cost-effective operations that are well-suited for large-scale manufacturing. Metal-bearing precursors can be produced in desired shapes by conventional deformation processing (e.g., rolling, forging, extrusion, pressing, etc.) or by melt processing. As discussed above, the volume change upon oxidation (and nitridation) can be quite uniform and small for finely-divided (or chemically-homogeneous), alkaline-earth-metal-bearing precursors.

Under appropriate conditions of mechanical alloying, the precursors can be malleable, so that organic additives (binder, plasticizer, etc.) are not required to produce a shaped body. Consequently, the defects generated by incomplete or inhomogeneous organic pyrolysis (cracks, delaminations, residual trapped carbon) can be avoided. Further, owing to the absence of carbon and the avoidance of CO/CO_2, H_2O, and gaseous hydrocarbons (associated with organic pyrolysis), the formation of intermediate carbonates or hydroxides can be prevented. As a result, novel reaction paths to multicomponent ceramics can be accessed. Since a finely-divided, highly-reactive mixture of precursor oxide phases can be produced by the oxidation of a

II. Introduction (cont.)

B. Attractive Features of the SMP Method (cont.)

finely-divided or chemically-homogeneous metal-bearing precursor, a multicomponent ceramic phase can be formed at reduced temperatures. For example, by avoiding the formation of the relatively stable carbonate, $BaCO_3$, multicomponent oxides such as $YBa_2Cu_3O_{7-y}$, Ba_2TiO_4, $BaAl_2O_4$, and $BaCeO_3$ have started forming within oxidized metal-bearing precursors at ≤550°C [5, 7, 12, 50].

Sintering of ceramic bodies produced by the SMP approach can occur at relatively low temperatures or in relatively short times. Oxide grains formed by oxidation at moderate temperatures (<900°C) tend to be quite fine (submicron - see Fig. 9b on page 17). Fine-grained, oxidized precursors can exhibit an enhanced rate of sintering. Since an intimate mixture of precursor oxide phases can be produced by the oxidation of multicomponent metal-bearing precursors, the rate of densification may be further enhanced by a reactive sintering process. Indeed, completely dense $YBa_2Cu_3O_{7-y}$/Ag composites have been formed by oxidizing melt-spun Y-Ba-Cu-Ag ribbons at 500°C and then annealing for 5 hours at 900°C [13]. Dense $BaTiO_3$/Pd laminates have also been produced by oxidizing Ba-Ti/Pd metallic precursor laminates at ≤900°C, and then annealing for 10 hrs at 1085°C (without the use of a liquid-phase sintering aid!) [1]. Dense $BaCeO_3$ tapes have been produced after oxidation and annealing of Ba-CeH_3 precursors at a peak temperature of 900°C [7]. $YBa_2Cu_3O_{7-y}$/Ag composites, $BaTiO_3$/Pd laminates, and $BaCeO_3$ bodies prepared by more conventional processing routes require significantly longer times or higher temperatures for complete densification without the use of sintering aids. Oxidation and densification at relatively low temperatures are desired to reduce processing costs of ceramic composites and to minimize fiber-matrix reactions.

In summary, under appropriate conditions of processing, malleable alkaline-earth-metal-bearing precursors can be deformed or cast into desired shapes, oxidized rapidly, transformed into a multicomponent ceramic compound (or compounds) at modest temperatures, and sintered to high density to yield a near net-shaped ceramic body. Work over the past year in the present program has demonstrated that such features also apply to the syntheses of celsian and celsian-matrix composites from solid, metal-bearing precursors.

III. Results and Discussion

The work conducted from April 15, 1994 to April 14, 1995 has been focused in the following areas:

1) Understanding the intermediate reactions leading to monolithic celsian
2) Evaluating the feasibility of synthesizing celsian-matrix composites
3) Demonstrating the near net-shape feature of the SMP process

SEM, EPMA, TEM, and XRD analyses have been used to evaluate the reaction paths to celsian from various precursors (i.e., all metallic, metal/oxide). The influence of dopants (strontium, magnesium) on the formation of monolithic celsian has also been studied. The SMP method has been applied to the syntheses of celsian/zirconia, celsian/alumina, and celsian/silicon nitride composites. Near net-shaped monolithic celsian and celsian-zirconia composites have also been produced. Progress in these areas is presented in this section of the report.

A. Synthesis of Monolithic Celsian

1. All-Metallic Precursors (Ba-Al-Si)

a) Precursor Preparation

Ba-Al-Si metallic precursor tapes were prepared by compaction and deformation of powders produced by solid-state mechanical alloying of the elements (see schema in Fig. 1). The starting elemental aluminum and silicon were powders, obtained from Goodfellow, Inc. (Malvern, PA),

III. Results and Discussion (cont.)

A. Synthesis of Monolithic Celsian (cont.)

1. All-Metallic Precursors (cont.)

a) Precursor Preparation (cont.)

with average particle sizes of ≈ 10 μm and ≈ 5 μm, respectively. The overall purities of the aluminum and silicon powders were >99% (major Al impurities: Si+Fe <0.9 wt%, Zn<0.1 wt%) and >97.5% (major Si impurities: Al<0.6 wt%, Ca<0.5 wt%, Fe<0.5 wt%), respectively. Elemental barium was obtained from Aldrich Chemical Co. (Milwaukee, WI) in the form of dense rods with purities of >99% (major impurities: Sr<0.76 wt%, Ca<0.12 wt%). Barium flakes (≈200 μm in length) were produced from the barium rods by filing with a seasoned steel file. All powder handling was conducted within an argon-atmosphere glove box.

An equimolar mixture of aluminum and silicon powder was placed within an o-ring sealed hardened steel vial, along with hardened steel balls and hexane as a milling lubricant. Milling was conducted within a high-energy vibratory ball mill (Model 8000 Mixer-Mill, SPEX Industries, Edison, NJ) for 4 hours. Barium flakes were then added to the milled powder to achieve a Ba:Al:Si molar ratio of 1:2:2, which was consistent with the desired ceramic compound, celsian ($BaAl_2Si_2O_8$). Additional milling was then conducted for 1 hour. An x-ray diffraction pattern of the resulting Ba-Al-Si powder revealed diffraction peaks for elemental barium, aluminum, and silicon. Intermetallic compounds, such as $BaAl_2Si_2$ [41], were not observed to have formed. A high volume fraction of intermetallic compounds was not desired, owing to complications in room-temperature compaction and deformation of such brittle phases.

After milling, the Ba-Al-Si powder mixture was sealed within evacuated, fugitive silver tubes with inner and outer diameters of 0.93 cm and 1.03 cm, respectively (99.9% purity, Handy and Harmon Co., E. Providence, RI) and rolled into tapes. Rolling was conducted at room temperature with a two-high rolling mill (8.5 cm dia. rolls) at a rate of ≈22 cm/sec. After every 50% reduction in thickness, the tape was annealed for 1 hour at 300°C in a vacuum oven, in order to prevent edge cracking of the silver tube. An optical micrograph of a cross-section of a tape is shown in Fig. 5. The compacted Ba-Al-Si core of the tape was quite malleable, as revealed by the absence of cracks and by the uniformity in the thickness of the core.

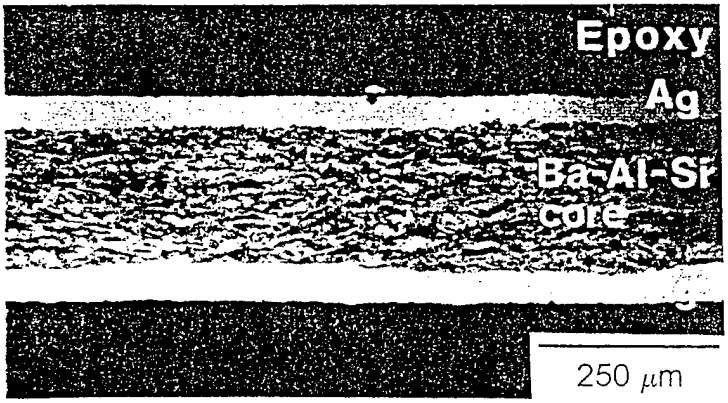

Figure 5. Optical micrograph of a longitudinal cross-section of a silver-sheathed Ba-Al-Si precursor tape produced by room-temperature rolling of mechanically-alloyed Ba-Al-Si powder.

III. Results and Discussion (cont.)

A. Synthesis of Monolithic Celsian (cont.)

1. All-Metallic Precursors (cont.)

b) Oxidation Processing

The silver-sheathed tapes were cut into 15 mm lengths and exposed to oxidation heat treatments conducted in flowing, purified oxygen[2] over a range of temperatures, as shown in Figs. 6b and 6c. In order to avoid the generation of a low-melting Ba-Ag eutectic liquid at 340°C [1, 51], the precursor tapes were given an initial oxidation treatment at 300°C in pure, flowing oxygen. Ag is sufficiently noble that it should remain metallic under these conditions, whereas the Ba should transform into oxide. The core of each tape was exposed only at the cut ends (see Fig. 6a), so that oxidation at this temperature proceeded inward from the ends of each specimen[3]. The oxidation cycle was then continued with constant temperature anneals at 500°C and 900°C. After the 900°C treatment, the fugitive silver sheath was cleanly peeled away from the oxidized core of the tape (silver melts at 939°C in pure oxygen at 1 atm pressure [52]). The core was then sandwiched between sheets of palladium foil, to avoid interaction with the ceramic boat upon which the specimen rested during higher temperature heat treatments. To allow for conversion of the oxidized tapes to $BaAl_2Si_2O_8$, an additional heat treatment step was conducted at 1200°C in the cycle shown in Fig. 6b. A second heat treatment cycle, containing anneals at 1100°C, 1200°C, and 1260°C (see Fig. 6c), was introduced to further elucidate the reactions leading to the monolithic polymorph of $BaAl_2Si_2O_8$.

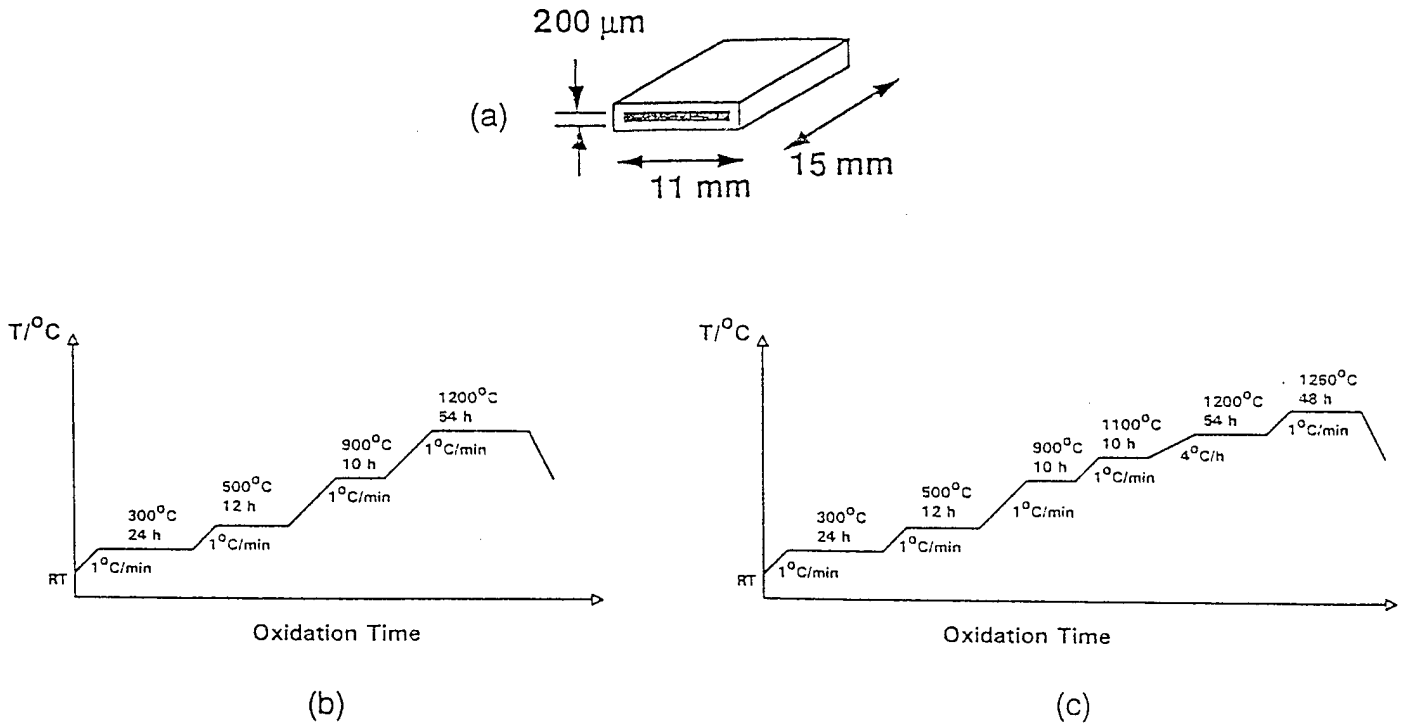

Figure 6. (a) Geometry of the silver-sheathed Ba-Al-Si specimens. (b), (c) Heat treatment cycles used to oxidize and transform the Ba-Al-Si precursors into $BaAl_2Si_2O_8$ (as discussed in the text, the silver sheath was removed after the 900°C stages of these thermal treatments).

---

2 The oxygen was passed through a drierite/ascarite column to remove residual water vapor or carbon dioxide.

3 Oxygen diffusion through silver at 300°C is sufficiently slow that the oxidation reaction at this temperature occurred by the propagation of an oxidation front from the ends of the tape (not through the silver sheath) [1].

III. Results and Discussion (cont.)

A. Synthesis of Monolithic Celsian (cont.)

1. All-Metallic Precursors (cont.)

b) Oxidation Processing (cont.)

Prolonged annealing times were chosen at each constant temperature stage of heat treatment to allow for more complete reaction and/or coarsening of resulting phases for subsequent detection by electron microscopy. For example, prior work on other Ba-bearing tape precursors has revealed that barium oxidation can be completed within 8 hours over a 15 mm length at 300°C [1, 2, 5], although 24 hours were used at this temperature in the present work.

c) Characterization Methods

After a given isothermal treatment, a specimen was air quenched and then characterized by x-ray diffraction (XRD) and electron microscopy. XRD analyses were conducted with Cu Kα radiation (Scintag PAD V system) at room temperature on powder prepared from the oxidized Ba-Al-Si core of tape specimens. Electron microprobe analyses (EPMA) were conducted on polished metallographic cross-sections of oxidized specimens with a Cameca SX 50 instrument. To allow for quantitative WDX analyses with the electron microprobe, calibrations were conducted for barium, aluminum, and silicon using barium titanium silicate, $BaTiSi_3O_9$[4], and anorthite, $CaAl_2Si_2O_8$[5], standards. EDX analyses were conducted with a Philips XL-30 SEM. EDX analyses were calibrated with reference to a BaO-Al_2O_3-SiO_2-bearing glass standard whose composition had been independently measured by wet chemical and spectrographic analyses (the standard composition was 33.92 wt% Ba, 14.34 wt% Al, 16.38 wt% Si, and 35.36 wt% O)[6]. Electron diffraction and energy-dispersive x-ray (EDX) analyses were conducted on thinned samples with a Philips CM200 TEM operating at 200 kV. Specimen cross-sections were glued within a 3 mm diameter stainless steel tube and thinned to perforation using standard grinding and ion milling procedures. A piece of the BaO-Al_2O_3-SiO_2-bearing glass standard used for EDX/SEM calibration was thinned to perforation for use as an EDX/TEM standard. Oxygen was not directly measured by quantitative EDX or WDX analyses. Instead, valences of +2, +3, and +4 were assumed for oxidized barium, aluminum, and silicon, respectively, to allow for calculation of the oxygen content.

Partially-transformed specimens (i.e., specimens oxidized at $\leq$900°C) were prone to reaction with water vapor or carbon dioxide present in ambient air. To avoid such reaction, the silver sheathing on partially-oxidized specimens was not removed until the specimens were transferred into the argon-atmosphere glove box after oxidation (only the cut ends of the silver-sheathed tapes were exposed to ambient air during this transfer). After removing the sheathing in the glove box, the partially-oxidized precursor core was ground into powder with an alumina mortar and pestle. The powder was then mixed with x-ray transparent grease (Dow Corning, Inc., Midland, MI) and placed on the XRD specimen holder (either polycrystalline silver or a silicon single crystal). The grease-coated powder was then removed from the glove box into ambient air and placed within the XRD system for characterization. The grease coating protected the partially-oxidized powder from excessive reaction with carbon dioxide and water vapor in air during XRD data collection. During grinding and polishing of partially-oxidized specimens for EPMA, mineral oil was used as a lubricant and sealant to avoid reaction with air. Just prior to coating of the polished specimen with carbon, the oil was removed from the specimen surface with hexane.

---

4 Obtained from Tousimis Research Corporation, Rockville, MD

5 Obtained from the Dept. of Mineral Science, Smithsonian Institute, Washington, DC

6 N. P. Bansal, NASA-Lewis Research Center, private communication

III. Results and Discussion (cont.)

A. Synthesis of Monolithic Celsian (cont.)

1. All-Metallic Precursors (cont.)

d) Phase and Microstructural Evolution

After exposure to O_2(g) a peak temperature of 300°C:

In order to determine whether the oxidation of barium at 300°C could be conducted over macroscopic distances within bulk Ba-Al-Si bodies, the sheathed Ba-Al-Si core within any given tape was directly exposed to oxygen only at the cut ends of the tape (see Fig. 6a). XRD spectra obtained from air-quenched specimens after various stages of the heat treatment cycle of Fig.6b are shown in Fig. 7. After exposure to flowing oxygen at 300°C for 24 hours, predominant peaks were detected for barium peroxide (BaO_2), aluminum, and silicon. Diffraction peaks for elemental barium, and for alumina and silica, were not detected. This indicates that barium oxidation was completed, whereas much of the aluminum and silicon remained unoxidized, within the 15 mm long, silver-sheathed tapes after exposure to oxygen for 24 hours at 300°C. Relatively small peaks for barium orthosilicate, Ba_2SiO_4, were also detected in the specimen quenched from 300°C.

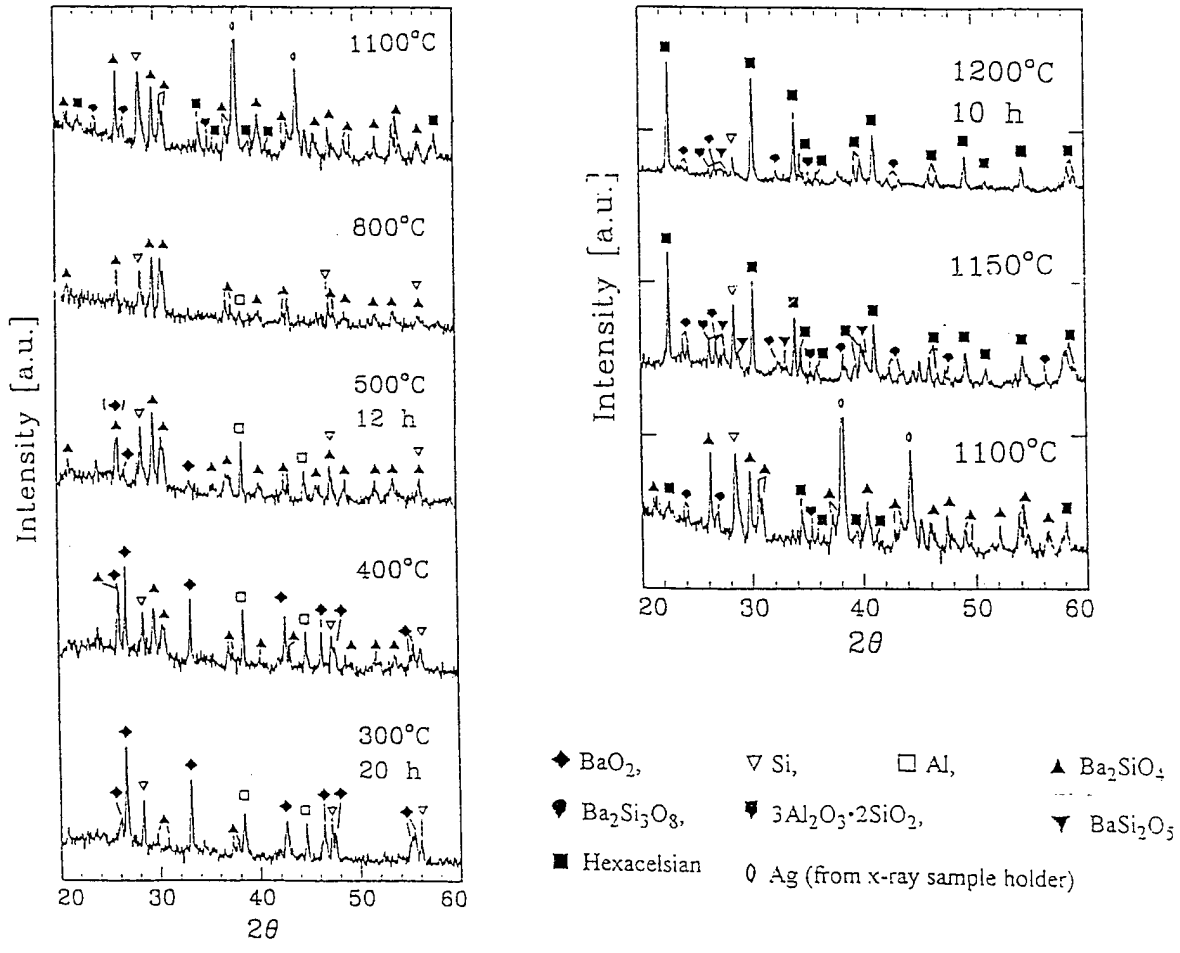

Figure 7. XRD spectra taken from the powderized core of Ba-Al-Si tape specimens that were air quenched after heat treatment in flowing oxygen at peak temperatures ranging from 300 to 1200°C (using the heat treatment cycle shown in Fig. 6b). The 800°C, 1100°C, and 1150°C spectra were obtained from samples quenched during heatup between isothermal anneals.

III. Results and Discussion (cont.)

A. Synthesis of Monolithic Celsian (cont.)

1. All-Metallic Precursors (cont.)

d) Phase and Microstructural Evolution (cont.)

A backscattered electron image of a polished cross-section of a specimen exposed for 20 hours at 300°C is shown in Fig. 8a. Associated x-ray dot maps for barium, aluminum, silicon, and oxygen are shown in Figs. 8b-e. The x-ray maps indicated that the dark phases in the BSE image were enriched in either silicon or barium and depleted in oxygen (some dark pores were also present). Quantitative EPMA revealed that these particles were elemental silicon (labeled S in Fig. 8a) and aluminum (labeled A in Fig. 8a). The aluminum particles were elongated in a direction approximately parallel to the direction of rolling. The oxygen map revealed that the barium-rich matrix (labeled B in Fig. 8a) surrounding these particles was oxidized, which is consistent with the detection of BaO_2 by XRD. Fine (≤10 μm) pores were detected within the interconnected BaO_2 phase after oxidation at 300°C. Such porosity may have provided a rapid diffusion path for oxygen during oxidation of the aluminum and silicon phases at the higher temperature stages of the heat treatment. The barium orthosilicate phase barely detected by XRD in the specimen annealed at 300°C for 24 hours could not be unambiguously detected in the specimen shown in Fig. 8a, presumably because of the small amount (or fine size) of this phase produced after 20 hours at 300°C.

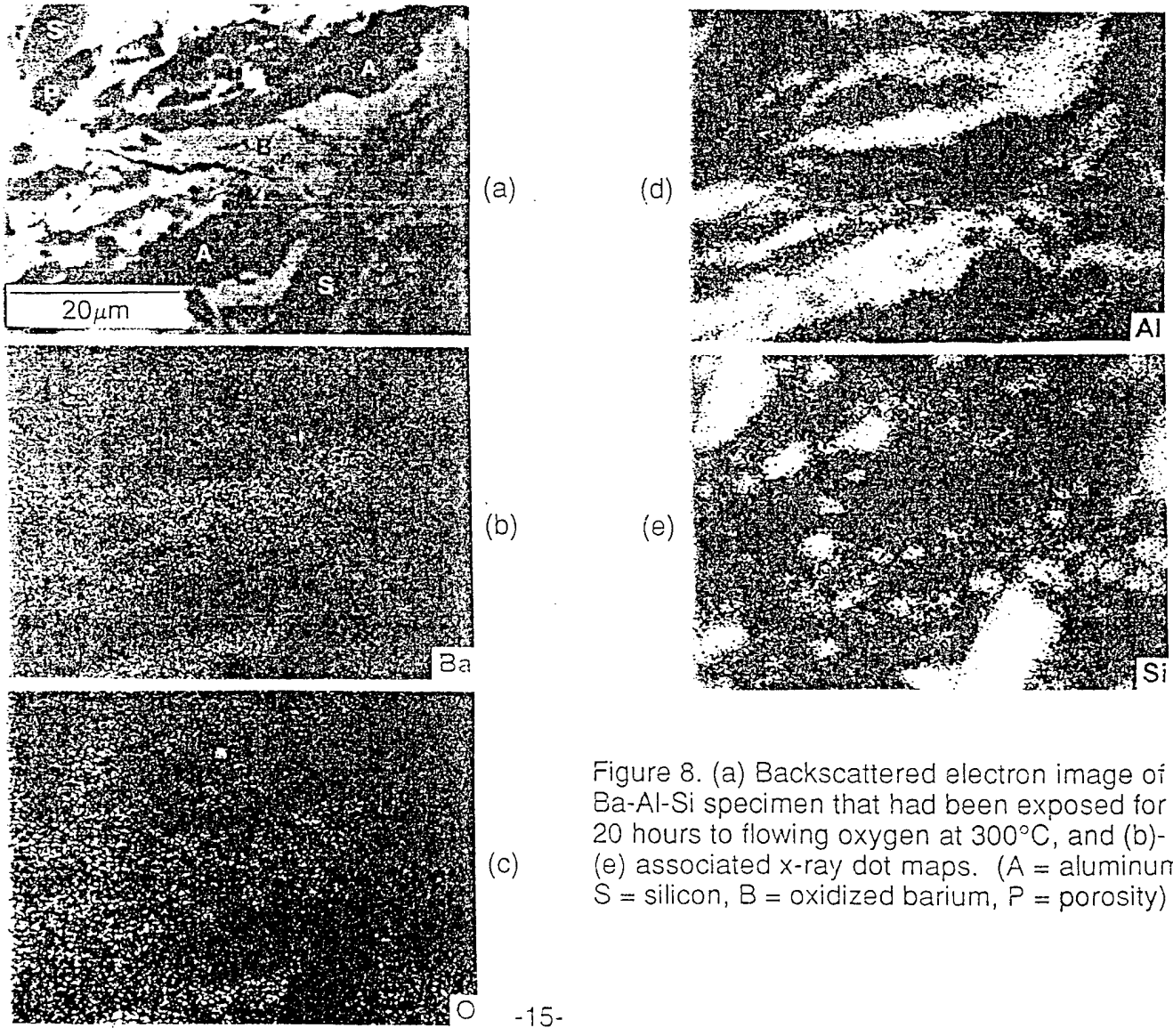

Figure 8. (a) Backscattered electron image of a Ba-Al-Si specimen that had been exposed for 20 hours to flowing oxygen at 300°C, and (b)-(e) associated x-ray dot maps. (A = aluminum, S = silicon, B = oxidized barium, P = porosity)

III. Results and Discussion (cont.)

A. Synthesis of Monolithic Celsian (cont.)

1. All-Metallic Precursors (cont.)

d) Phase and Microstructural Evolution (cont.)

The complete oxidation of barium in the 15 mm long Ba-Al-Si tapes at 300°C was not particularly surprising. At modest temperatures, barium and other alkaline earth metals have been observed to oxidize at relatively rapid linear rates [43-49]. Such rapid, linear oxidation has been attributed to the presence of an open network of pores generated as a result of the smaller molar volume of barium oxide(s) relative to the molar volume of metallic barium ($V_m(BaO_2) < V_m(Ba)$) [44]. Thermodynamic data compiled by Barin and Knacke, et al. [53, 54] indicates that the exposure of barium to pure oxygen at 300°C should result in the formation of barium peroxide. However, barium peroxide is not stable in contact with elemental silicon or aluminum; that is, red-ox reactions between silicon or aluminum and barium peroxide, such as shown below, are thermodynamically possible:

$$Si + 2\ BaO_2 \Rightarrow 2\ BaO + SiO_2 \qquad (2a)$$

or

$$Si + 2\ BaO_2 \Rightarrow Ba_2SiO_4 \qquad (2b)$$

$$2\ Al + 3\ BaO_2 \Rightarrow 3\ BaO + Al_2O_3 \qquad (3a)$$

or

$$2\ Al + 3\ BaO_2 \Rightarrow Ba_3Al_2O_6 \qquad (3b)$$

Apparently, the rate of formation of BaO_2 (by reaction with gaseous oxygen) was much faster than the rates of these red-ox reactions at ≤300°C.

After exposure to $O_2(g)$ at peak temperatures of 400°C-500°C:

The XRD pattern of a specimen quenched from 400°C (during the 1°C/min heatup from 300 to 500°C) revealed peaks for similar phases as had been detected from the sample quenched at 300°C, although the diffraction peaks for Ba_2SiO_4 were appreciably larger (Fig. 7). After further heat treatment for 12 hours at 500°C, the relative heights of Ba_2SiO_4 peaks had continued to increase, whereas the peaks for BaO_2 had nearly vanished. The nearly complete consumption of BaO_2 to form Ba_2SiO_4 indicated that about one-fourth (by mole fraction) of the silicon in the precursor was oxidized within 12 hours at 500°C. Diffraction peaks for residual, unoxidized aluminum and silicon were also detected in the 500°C specimens.

While the amount of Ba_2SiO_4 was clearly observed to increase as heat treatment proceeded from 300°C to 500°C, diffraction peaks for crystalline BaO and SiO_2 were not detected in specimens quenched from this temperature range. This suggested that: 1) crystalline BaO and SiO_2 were present as short-lived intermediates to Ba_2SiO_4 (i.e., at any particular time at 400-500°C, BaO and SiO_2 were present at volume fractions too low to be detected by XRD), or 2) Ba_2SiO_4 was directly produced by the reaction of BaO_2 with Si, or 3) that amorphous or nanocrystalline baria and/or silica-bearing phases preceded the formation of Ba_2SiO_4.

In order to determine whether crystalline BaO and SiO_2 were present as intermediate phases prior to the formation of Ba_2SiO_4, TEM analyses were conducted on a specimen quenched from 400°C. Bright-field TEM images are shown in Figs. 9a-c and a high-resolution image is shown in Fig. 9d. EDX analyses confirmed the presence of elemental silicon and aluminum, along with Ba_2SiO_4, as shown in Figs. 9a-d. The Ba_2SiO_4 phase was polycrystalline and possessed a very fine grain size (on the order of 30 nm) as shown in Fig. 9b. EDX analyses also confirmed the presence of a barium-rich phase depleted of aluminum and silicon (labeled Ba/X in Fig. 9a and Ba/O/C in Fig. 9c)), although selected area electron diffraction patterns were not consistent with BaO_2. Because this specimen was exposed to air during transfer from the

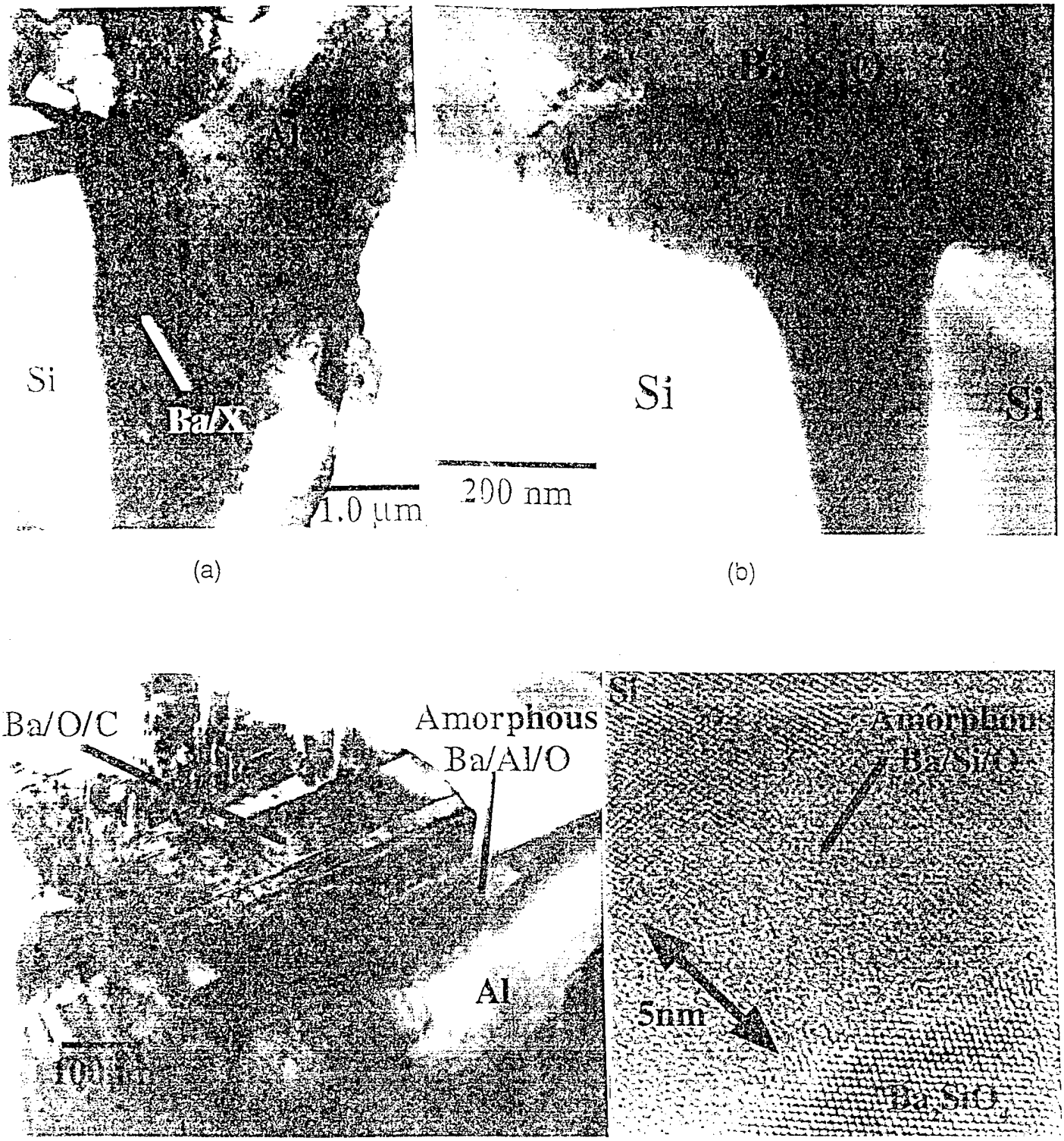

Figure 9. (a)-(c) Bright field TEM images and (d) a high resolution image of a Ba-Al-Si specimen that had been quenched after exposure for 24 hours at 300°C, and then heating at 1°C/min to 400°C (all in flowing oxygen).

III. Results and Discussion (cont.)

A. Synthesis of Monolithic Celsian (cont.)

1. All-Metallic Precursors (cont.)

d) Phase and Microstructural Evolution (cont.)

ion mill to the TEM, it is likely that BaO_2 originally present in the specimen had reacted with carbon dioxide or water vapor to form a carbonate, hydroxide, or hydroxycarbonate (in fact, some carbon was detected in the Ba/O/C phase by EDX analysis). The key TEM observations for this specimen are with regard to phases present at interfaces between the Si or Al particles and the Ba-O-bearing grains. In Fig. 9d, a high-resolution image reveals a very thin amorphous phase ($\approx$ 5 nm thick, labeled Ba/Si/O) located at the interface between Si and Ba_2SiO_4. EDX analysis revealed that this phase contained barium, silicon, and oxygen. A layer of pure SiO_2 was not detected between silicon and the Ba-Si-O glass. Hence, while the steady-state reaction of BaO_2 with Si to form Ba_2SiO_4 appears to involve the formation of a glassy silicate, pure silica was apparently not involved as an intermediate phase.

The bright-field TEM image in Fig. 9c reveals a boundary between an Al particle and Ba-O-C bearing grains (the latter was presumed to have been BaO_2 prior to exposure to air). Electron diffraction and EDX analyses have revealed that the phase located between the Al and Ba-O-C bearing grains consisted of an amorphous phase containing Ba, Al and O. A layer of pure, crystalline Al_2O_3 was not detected between aluminum and the Ba-Al-O-bearing glass. Hence, TEM analyses revealed that Ba-Al-O-bearing glass could be produced by the direct reaction of BaO_2 with Al (i.e., crystalline Al_2O_3 formation was apparently not required). TEM analyses of several thinned regions indicated that the amount of the Ba-Al-O-bearing glass produced at 400°C was considerably less than the amount of crystalline Ba_2SiO_4 produced by the reaction of BaO_2 with Si, which explains the lack of detection of the Ba-Al-O-bearing glass by EPMA.

After exposure to O_2(g) at peak temperatures of 700°C-800°C:

After further exposure to O_2(g) during heat up between 500°C and 800°C, the diffraction peaks for elemental aluminum nearly vanished (Fig. 7). Predominant peaks for Ba_2SiO_4 and elemental silicon remained. XRD analyses did not reveal the presence of BaO_2 (or BaO), Al_2O_3, SiO_2, or other oxide phases. A backscattered electron image and associated x-ray dot maps of a specimen exposed to a peak temperature of 700°C (i.e., quenched during the heatup between 500 and 900°C) are shown in Figs. 10a-e. Several dark particles, that were rich in either aluminum or silicon, were contained in a brighter, barium-rich matrix. The silicon-rich particles (labeled S in Fig. 10a) were clearly depleted of oxygen. WDX analyses of relatively large (>5 μm in diameter) silicon-rich particles confirmed that these particles were largely unoxidized. The measured composition of the bright barium-rich matrix phase (labeled B_2S in Fig. 10a) was 77.4 wt% BaO + 22.6 wt% SiO_2, which is similar to the composition of Ba_2SiO_4 (83.6 wt% BaO + 16.4 wt% SiO_2). Hence, the presence of silicon and Ba_2SiO_4 after oxidation at up to 700-800°C was confirmed by both XRD and EPMA. The aluminum-rich particles (labeled AO in Fig. 10a) were too fine to allow for unambiguous identification by EPMA. Nonetheless, the lack of clear oxygen depletion in these and other aluminum-rich particles, and the significant decline in the height of diffraction peaks for aluminum in this temperature range indicated that the aluminum-rich particles were composed of Al_2O_3. (The absence of detectable diffraction peaks for Al_2O_3 in Fig. 7 could be attributed to the relatively low x-ray scattering associated with this compound relative to Ba_2SiO_4.)

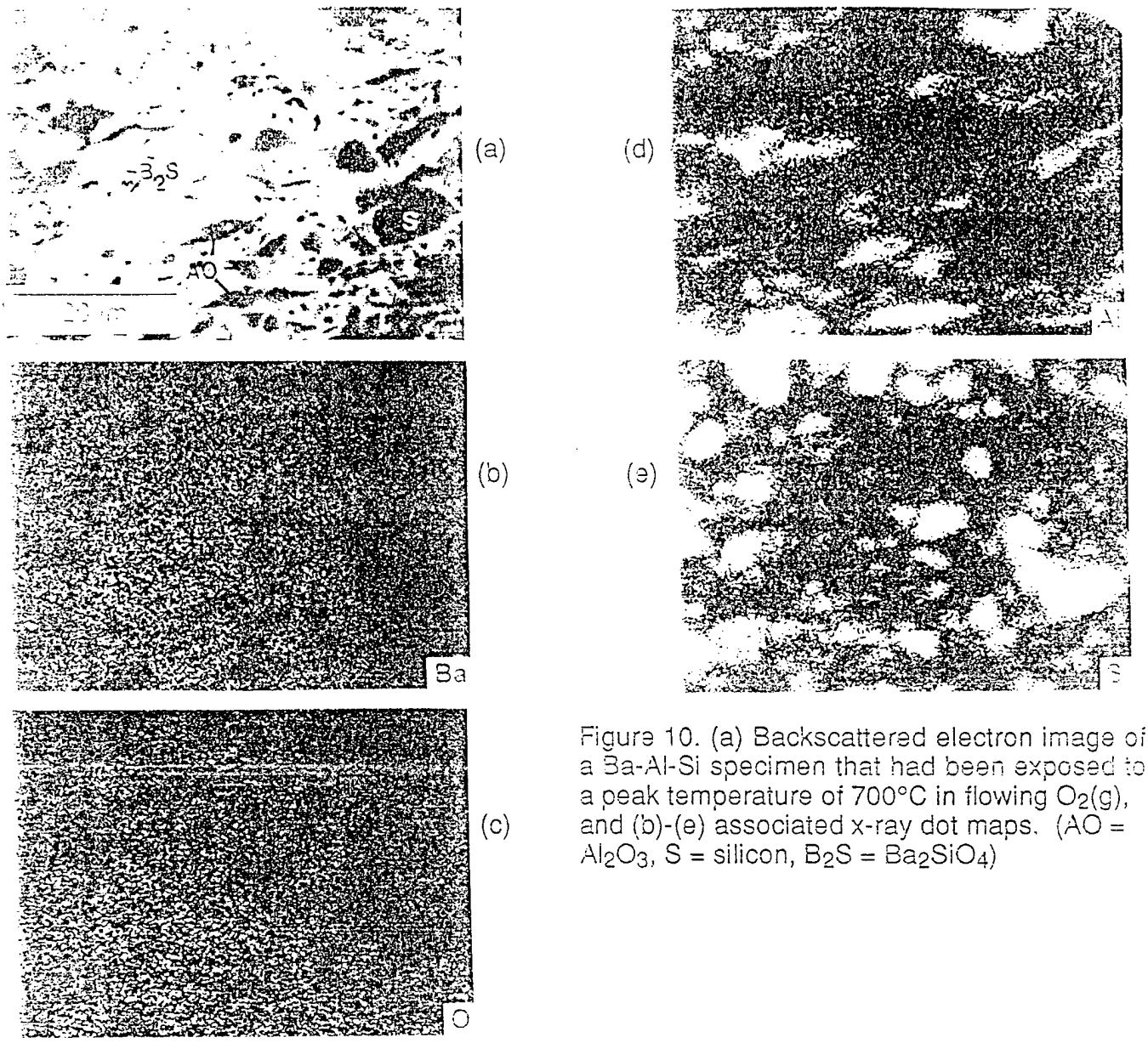

Figure 10. (a) Backscattered electron image of a Ba-Al-Si specimen that had been exposed to a peak temperature of 700°C in flowing $O_2(g)$, and (b)-(e) associated x-ray dot maps. (AO = Al_2O_3, S = silicon, B_2S = Ba_2SiO_4)

After exposure to $O_2(g)$ at peak temperatures of 1100°C-1260°C:

XRD analyses revealed that heating from 900 to 1100°C at 1°C/min resulted in the formation of small amounts of $Al_6Si_2O_{13}$ (mullite), $Ba_2Si_3O_8$, and the hexacelsian polymorph of $BaAl_2Si_2O_8$[7]. Residual silicon and Ba_2SiO_4 were also detected at 1100°C. Further heating at 1°C/min to 1150°C resulted in complete consumption of Ba_2SiO_4 and considerable formation of hexacelsian, although a fair amount of unreacted silicon remained. After 10 hours at 1200°C, much of the silicon had oxidized and hexacelsian had become the dominant phase. Small diffraction peaks were also attributed to residual mullite, $Ba_2Si_3O_8$, and $BaSi_2O_5$.

A backscattered electron image and associated x-ray dot maps of a specimen exposed to flowing oxygen for 10 hours at a peak temperature of 1200°C are shown in Figs. 11a-e. WDX analysis of the gray matrix phase (labeled BAS_2 in Fig. 11a) yielded a composition of 40.9 wt%

7 Diffraction lines for silver, observed in the XRD pattern of a specimen quenched from 1100°C (Fig. 7), were produced from a silver specimen holder used for this XRD analysis.

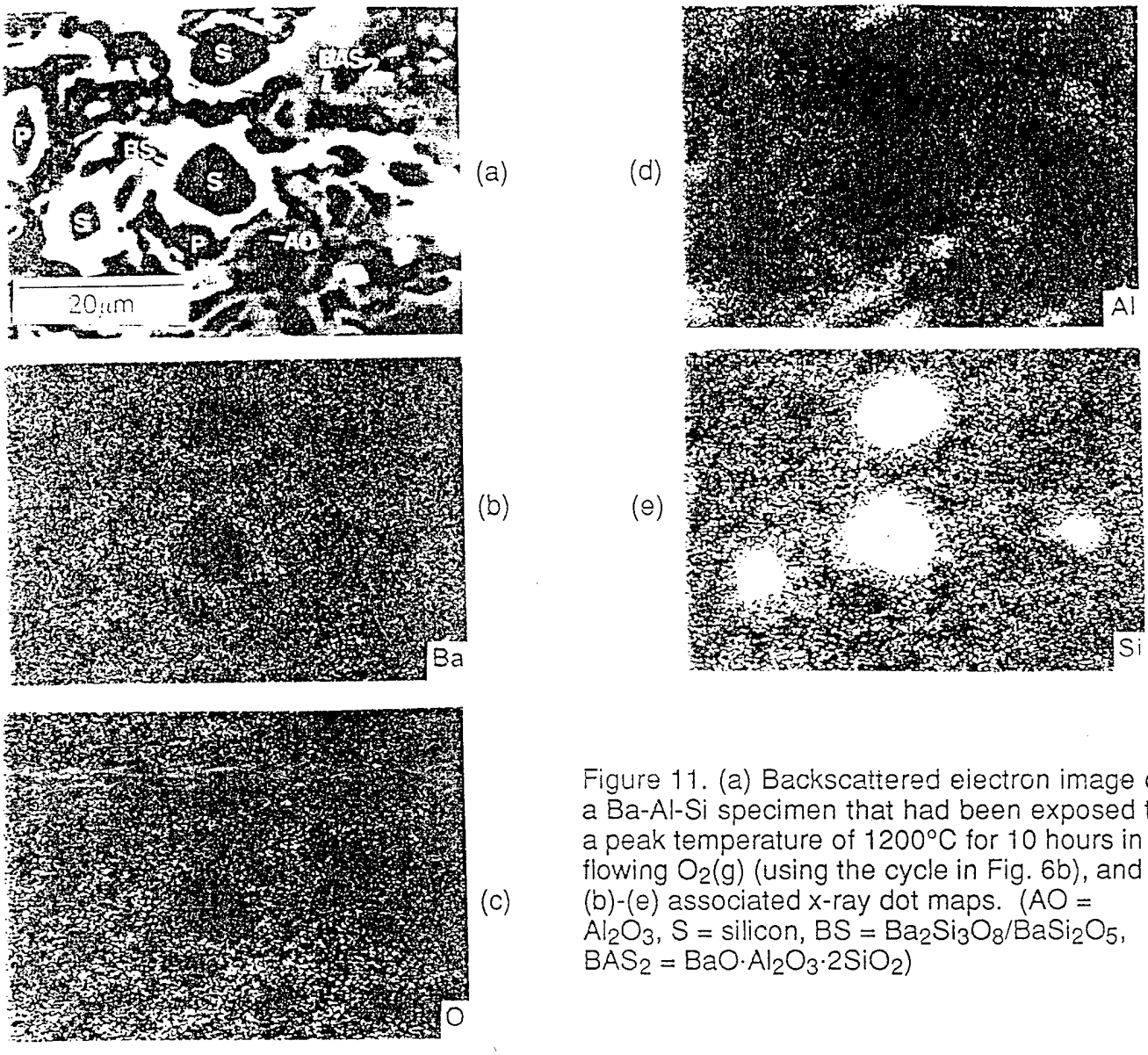

Figure 11. (a) Backscattered electron image of a Ba-Al-Si specimen that had been exposed to a peak temperature of 1200°C for 10 hours in flowing O_2(g) (using the cycle in Fig. 6b), and (b)-(e) associated x-ray dot maps. (AO = Al_2O_3, S = silicon, BS = $Ba_2Si_3O_8$/$BaSi_2O_5$, BAS_2 = $BaO{\cdot}Al_2O_3{\cdot}2SiO_2$)

BaO + 27.2 wt% Al_2O_3 + 32.0 wt% SiO_2, which is nearly identical to that for $BaAl_2Si_2O_8$ (40.8 wt% BaO + 27.2 wt% Al_2O_3 + 32.0 wt% SiO_2). Comparison with the XRD analyses in Fig. 7 suggested that this phase was hexacelsian. Dark particles (labeled S) were observed in Fig. 11a to be surrounded by a bright skin (labeled BS). The x-ray dot maps in Figs. 11b-e and subsequent WDX analyses revealed that the dark particles were composed largely of unoxidized silicon. The BS phase contained a relatively high barium content (see barium dot map in Fig. 11), and was depleted in aluminum. WDX analyses of several BS grains yielded an average composition of 58.2 wt% BaO + 41.8 wt% SiO_2, which falls between the compositions of the two binary barium silicates detected by XRD analyses: $Ba_2Si_3O_8$ (63.0 wt% BaO + 37.0 wt% SiO_2) and $BaSi_2O_5$ (56.1 wt% BaO + 43.9 wt% SiO_2). Several fine aluminum-rich particles (labeled AO in Fig. 11a) depleted of barium and silicon were also detected and were presumed (for similar reasons as discussed above) to be Al_2O_3.

III. Results and Discussion (cont.)

A. Synthesis of Monolithic Celsian (cont.)

1. All-Metallic Precursors (cont.)

d) Phase and Microstructural Evolution (cont.)

The formation of barium silicates as intermediate reaction products preceding the formation of $BaAl_2Si_2O_8$ has also been observed by other authors. Planz and Muller-Hesse produced $BaAl_2Si_2O_8$ by reacting a mixture of barium carbonate, amorphous silicic acid, and γ-alumina [55]. During heating, $BaSiO_3$ was the first silicate to form, followed by a series of silicates with higher silica contents until $BaSi_2O_5$ was produced. The reaction of $BaSi_2O_5$ with alumina then yielded hexacelsian. These authors also suggested that some amount of alumina may have been incorporated into $BaSi_2O_5$ prior to the formation of celsian, although existing BaO-Al_2O_3-SiO_2 phase diagrams do not reveal appreciable solid solubility of Al_2O_3 within $BaSi_2O_5$ [21, 22].

After realizing that hexacelsian formation commenced at about 1100°C, a second heat treatment cycle (shown in Fig. 6c) was conducted with an isothermal anneal for 10 hours at 1100°C and a particularly slow ramp from 1100 to 1200°C (4°C/hour). XRD analyses of samples quenched after 3 hours at 1200°C, 54 hours at 1200°C, and 48 hours at 1260°C are shown in Fig. 12. The increased amount of annealing time spent between 1100 and 1200°C resulted in nearly pure hexacelsian, as revealed by the XRD pattern of the specimen quenched after 3 hours at 1200°C (i.e., compare the XRD pattern after 10 hours at 1200°C in Fig. 7 with the pattern after 3 hours at 1200°C in Fig. 12). During further exposure for a total of 54 hours at 1200°C, conversion of some of the hexacelsian to monoclinic celsian occurred. After the final anneal for 48 hours at 1260°C, XRD-pure monoclinic celsian was produced. A backscattered electron image and associated x-ray dot maps of a specimen exposed for 48 hours at 1260°C are shown in Figs. 13a-e. The dot maps revealed a uniform distribution of barium, aluminum, silicon, and oxygen in this sample (note: the extensive cracking observed in this particular sample was a result of poor specimen handling and polishing). WDX analyses revealed the presence of $BaAl_2Si_2O_8$, consistent with XRD data.

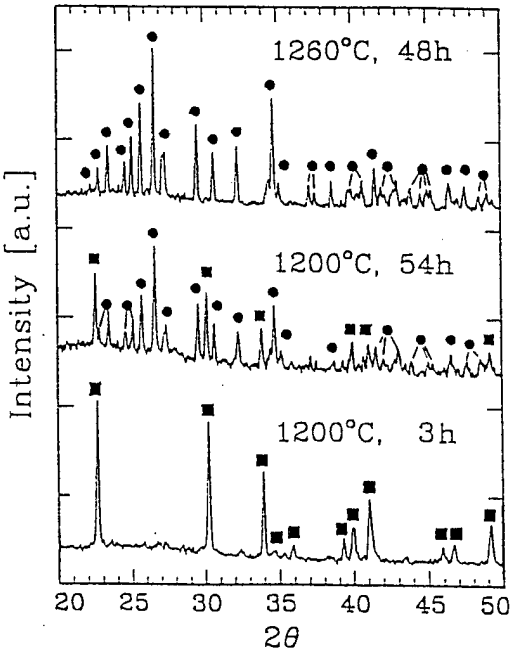

Figure 12. XRD spectra taken from the powderized core of Ba-Al-Si tape specimens that were air quenched after heat treatment in flowing oxygen at peak temperatures ranging from 1200°C to 1260°C (i.e., at various stages of the heat treatment cycle shown in Fig. 6c). ■ = hexacelsian, ● = monoclinic celsian.

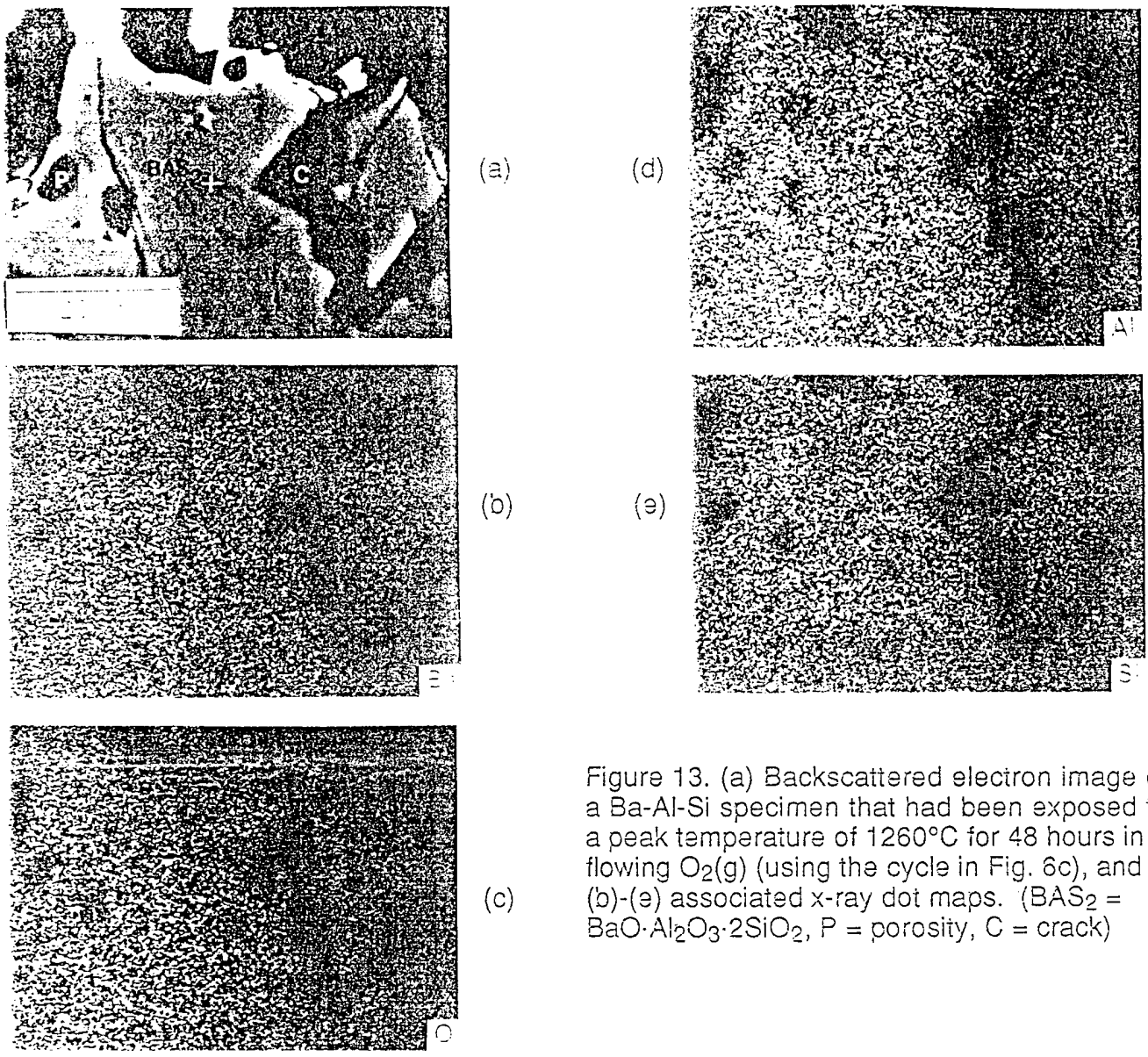

Figure 13. (a) Backscattered electron image of a Ba-Al-Si specimen that had been exposed to a peak temperature of 1260°C for 48 hours in flowing O_2(g) (using the cycle in Fig. 6c), and (b)-(e) associated x-ray dot maps. (BAS_2 = $BaO{\cdot}Al_2O_3{\cdot}2SiO_2$, P = porosity, C = crack)

The formation of metastable hexacelsian prior to monoclinic celsian has been observed by a number of authors upon heat treatment of a variety of crystalline or amorphous precursors [55-68]. In the absence of fluxing agents (e.g., LiF, Li_2O, CaF_2 [23, 56, 61-65, 68]) or solid-solution dopants (e.g., Sr, Ga, Ge substitutions for Ba, Al, and Si, respectively [64, 69-72]), the transformation of hexacelsian to monoclinic celsian proceeds at a very slow rate below 1590°C (the temperature above which hexacelsian is thermodynamically stable). For example, Chen, et al. [61, 63] observed that the conversion of hexacelsian to celsian in crystallized $BaO{-}Al_2O_3{-}SiO_2$ glass (produced from gel-derived precursors) required anneals of ≈28 days (≈670 hours) at 1320°C. In the present work, XRD-pure monoclinic celsian was produced from hexacelsian at a more rapid rate (i.e., within a total exposure time of 102 hours) within the temperature range of 1200-1260°C.

In order to better understand the hexacelsian-to-monoclinic celsian transformation in the oxidized SMP samples, TEM analyses were conducted on a partially-transformed specimen that,

according to XRD analysis, consisted of a mixture of only hexacelsian and monoclinic celsian. Bright field TEM images of two thinned regions produced from such a specimen that had been exposed for 30 hours at a peak temperature of 1200°C (by the cycle shown in Fig. 6c) are shown in Figs. 14a and 14b. In Fig. 14b, a relatively large, rectangular-shaped grain (labeled $BaAl_2Si_2O_8$) was observed. Finer grains of more spherical shape can be seen in Figs. 14a and 14b. EDX analyses revealed that both the spherical and rectangular shaped grains were composed of $BaAl_2Si_2O_8$. Selected area electron diffraction also revealed the presence of amorphous phases in Figs. 14a and 14b. EDX analyses of the amorphous phase yielded compositions that were near the 1200°C liquidus surface of the BaO-Al_2O_3-SiO_2 phase diagram, as shown in Fig. 15 [21, 22]. (The measured compositions of the $BaAl_2Si_2O_8$-type phase are also shown in this figure.) This suggests that some liquid oxide was present within the oxidized Ba-Al-Si specimens at ≥1200°C. The amorphous phase had not been previously detected by EPMA, which indicates that the overall amount of this phase (and, hence, the amount of liquid oxide present after 30 hours at 1200°C) was relatively small. While the exact mechanism of conversion of hexacelsian to monoclinic celsian is not yet clear, a liquid oxide phase may have assisted in this transformation (i.e. via a dissolution/reprecipitation mechanism).

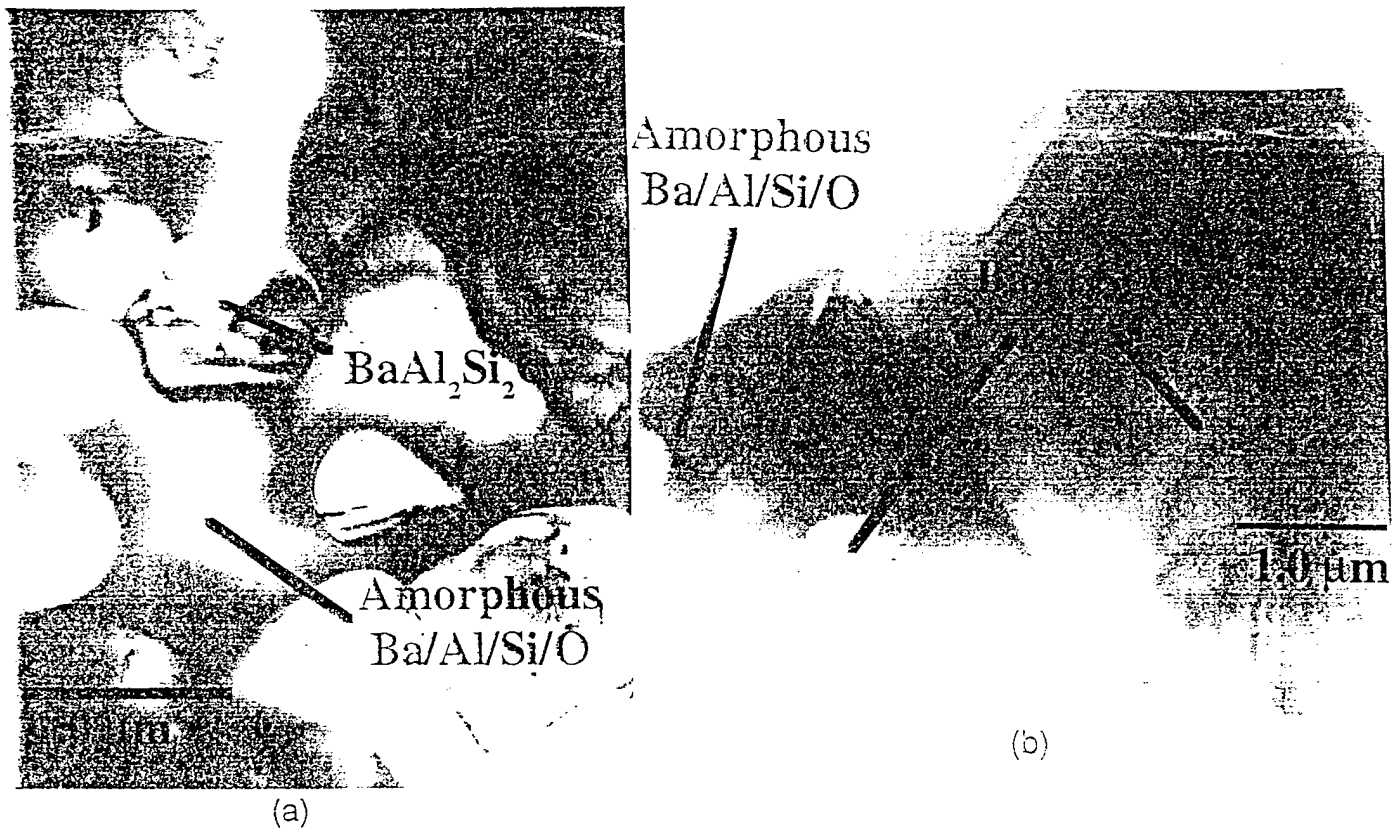

Figure 14. Bright field TEM images of a specimen quenched after 30 hours exposure to oxygen at 1200°C (the heat treatment cycle shown in Fig. 6c was used). The compositions measured by EDX of the amorphous phase and the crystalline grains are shown in Fig. 15.

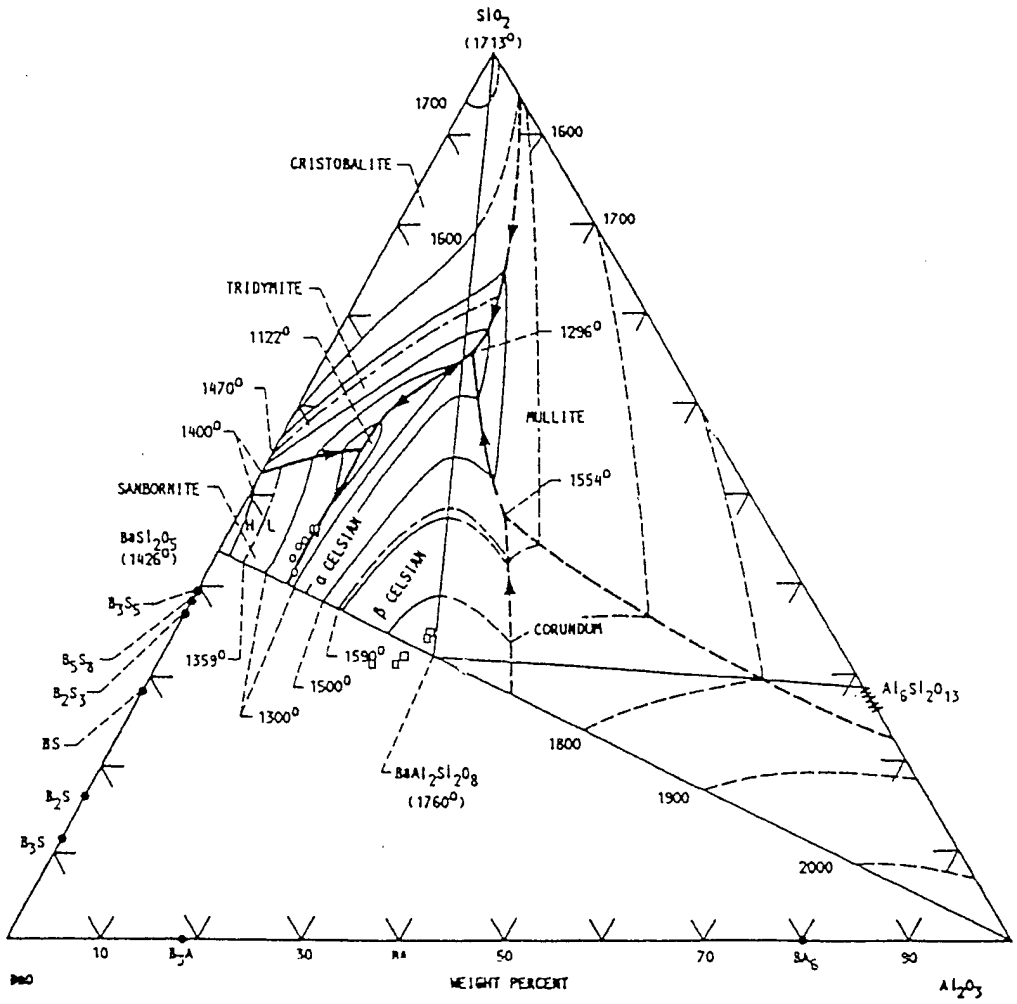

Figure 15. Compositions of the amorphous phase (open circles) and the $BaAl_2Si_2O_8$-type grains (open squares) measured by quantitative EDX/TEM analyses of a specimen quenched after heat treatment at a peak temperature of 1200°C for 30 hours in flowing oxygen (using the heat treatment cycle shown in Fig. 6b).

A summary of the phases detected at various stages of heat treatment of the Ba-Al-Si precursors is shown in Table 2 below.

Table 2. Phase Evolution to Celsian from Ba-Al-Si Precursors

Temperature/Time/Cycle			Phases Detected	Detection Method*
300°C	20 hours	1†	BaO_2	XRD, WDX
			Si	XRD, WDX
			Al	XRD, WDX
			Ba_2SiO_4	XRD
400°C	heatup#	1	Ba-O+	EDX
			Si	XRD, EDX
			Al	XRD, EDX
			Ba_2SiO_4	XRD, EDX, ED
			Ba-Al-O glass	EDX, ED
			Ba-Si-O glass	EDX, ED
500°C	12 hours	1	Ba_2SiO_4	XRD
			Si	XRD
			Al	XRD
			BaO_2	XRD

III. Results and Discussion (cont.)

A. Synthesis of Monolithic Celsian (cont.)

1. All-Metallic Precursors (cont.)

d) Phase and Microstructural Evolution (cont.)

Table 2. Phase Evolution to Celsian from Ba-Al-Si Precursors (cont.)

Temperature/Time/Cycle			Phases Detected	Detection Method*
700°C	heatup#	1	Ba_2SiO_4	WDX
			Si	WDX
			Al_2O_3	WDX
800°C	heatup#	1	Ba_2SiO_4	XRD
			Si	XRD
1100°C	heatup#	1	Ba_2SiO_4	XRD
			Si	XRD
			$Ba_2Si_3O_8$	XRD
			$Al_6Si_2O_{13}$	XRD
			hex-$BaAl_2Si_2O_8$	XRD
1150°C	heatup#	1	hex-$BaAl_2Si_2O_8$	XRD
			Si	XRD
			$BaSi_2O_5$	XRD
			$Ba_2Si_3O_8$	XRD
			$Al_6Si_2O_{13}$	XRD
1200°C	10 hours	1	hex-$BaAl_2Si_2O_8$	XRD, WDX
			Si	XRD,
			$BaSi_2O_5$	XRD, WDX
			$Ba_2Si_3O_8$	XRD, WDX
			$Al_6Si_2O_{13}$	XRD
			Al_2O_3	WDX
1200°C	3 hours	2	hex-$BaAl_2Si_2O_8$	XRD
1200°C	30 hours	2	$BaAl_2Si_2O_8$	EDX
			Ba-Al-Si-O glass	EDX, ED
1200°C	54 hours	2	hex-$BaAl_2Si_2O_8$	XRD
			mono-$BaAl_2Si_2O_8$	XRD
1260°C	48 hours	2	mono-$BaAl_2Si_2O_8$	XRD, WDX

* WDX= wavelength-dispersive x-ray analysis (quantitative analyses or qualitative x-ray dot maps) via EPMA, EDX= energy-dispersive x-ray analysis via TEM, ED= electron diffraction

\# Quenched during heatup at 1°C/min from 300-500°C, 500-900°C, or 900-1200°C.

‡ Presumed to have been BaO_2 prior to reaction with $H_2O(g)$ and $CO_2(g)$ in ambient air.

† Cycles 1 and 2 refer to the heat treatments shown in Figs. 6b and 6c, respectively.

e. Dimensional Changes

Metallographic measurements of the Ba-Al-Si precursor tape before and after transformation to celsian revealed an average change in thickness of +9.5% ($100 \cdot \Delta t/t_{precursor}$, where t refers to thickness). Consider the following net reaction.

$$Ba + 2\,Al + 2\,Si \xrightarrow[+\,O_2(g)]{heat} BaAl_2Si_2O_8 \text{ (monoclinic celsian)} \qquad (4)$$

III. Results and Discussion (cont.)

A. Synthesis of Monolithic Celsian (cont.)

1. All-Metallic Precursors (cont.)

e. Dimensional Changes (cont.)

The predicted thickness change for a Ba-Al-Si precursor (based on the molar volumes of barium, silicon, aluminum, and monoclinic celsian) undergoing this net reaction is 10.4%[8], which is in reasonable agreement with the measured thickness change. In order to obtain smaller dimensional changes after complete transformation to monoclinic celsian, precursors containing an appropriate mixture of metal and oxide phases need to be synthesized. Such precursors are discussed in the following section.

2. Oxidation of Metal/Oxide Precursors

Metal-oxide composite precursors are required in order to fabricate near net-shaped celsian and celsian composites by the SMP method. In this section of the report, the preparation of metal/oxide precursors, oxidation processing, phase/microstructural evolution are discussed. The fabrication of near net-shaped, phase-pure celsian bodies will also be described.

a) Precursor Preparation

Mechanical alloying was used to prepare metal-oxide precursor powder mixtures. The starting components are listed in Table 3 below.

Table 3. Starting Materials for Metal/Oxide Precursors

Material	Form	Ave. Size (μm)	Purity (%)	Commercial Source
Ba	Rods	not applicable	>99	Aldrich Chemical Co., Milwaukee, WI
Sr	Rods	not applicable	99.0	Johnson-Matthey, Ward Hill, MA
Mg	Powder	30	99.6	Cerac, Inc., Milwaukee, WI
α-Al_2O_3	Powder	1.5	99.99	Johnson-Matthey, Ward Hill, MA
Al	Powder	10	99.0	Goodfellow Corp., Malvern, PA
Si	Powder	2	99.9	Johnson-Matthey, Ward Hill, MA
SiO_2	Powder	2	98.8	Johnson-Matthey, Ward Hill, MA

The major impurities in the barium and strontium were other alkaline earth metals (e.g., for barium, the major impurities were ≤0.76 wt% Sr, ≤0.12 wt% Ca). The major impurities in the magnesium powder were ≤0.1% silicon, ≤0.05% manganese, and ≤0.03% iron. The major impurities in the aluminum powder were silicon and iron (≤0.9 wt% total of these elements). The major impurities in the silica (quartz) powder were alumina (≤0.4%), iron oxides (≤0.07%), potassia (≤0.06%) and calcia + magnesia (≤0.05%).

Ba and Sr flakes (≈200 μm in length) were produced by filing rods of these elements with a seasoned steel file. The cristobalite polymorph of silica was produced by heating the commercially-obtained quartz powder for 10 hours at 1600°C, followed by quenching and milling for 5 hours in a high-energy vibratory ball mill (the presence of crystobalite was confirmed by XRD). Ba-Al-αAl_2O_3-SiO_2(cristobalite) precursors with a targeted Ba: Al: Al_2O_3: SiO_2 molar ratio of 1.00: 1.68: 0.16: 2.00 were prepared. Such a precursor mixture was chosen such that

---

8 This predicted change in thickness is based on the assumption that the relative length change is the same in all three dimensions.

the reaction-induced volume change upon complete transformation to monoclinic celsian would be nearly zero (see discussion on pages 36 and 37). That is, the increase in molar volume due to aluminum oxidation was used to compensate for the decrease in molar volume due to barium oxidation. The oxidation of elemental silicon could also have been used to compensate for the decrease in molar volume due to barium oxidation; that is, Ba-Si-Al_2O_3-SiO_2 precursors with an appropriate amount of Ba and Si could also be used, in principle, to produce near net-shaped celsian. However, the aluminum in Ba-Al-Al_2O_3-SiO_2 precursors is more ductile than the silicon in Ba-Si-Al_2O_3-SiO_2 precursors, so that the former type of precursor should be more malleable than the latter. Hence, the transformation of Ba-Al-Al_2O_3-SiO_2 precursors was examined in more detail. Half of the barium (on a mole% basis) was replaced in some precursors with either strontium or magnesium in order to determine whether these dopants would enhance the formation of monoclinic celsian during later stages of heat treatment.

5-10 gram batches of these mixtures were placed in a yttria-stabilized zirconia vial (3.5 cm inner diameter, 4.5 cm length). Along with each powder mixture, 2 yttria-stabilized zirconia balls and 30 mL of hexane were added to the zirconia vial. The vial was then sealed in an argon-filled glove box and transferred to the high-energy vibratory SPEX mill. After milling, the zirconia vial was returned to the glove box whereupon the hexane was removed by filtration and evaporation. Milling of the precursor mixtures was conducted for relatively short times $\leq$4 hours, in order to avoid the formation of brittle intermetallic compounds (such as BaSi, $BaSi_2$, $BaAl_4$, Ba_7Al_{13}, $BaAl_2Si_2$ [41]). XRD patterns of the precursor powders indicated only the presence of the starting precursor components; that is, no peaks for intermetallic compounds were detected.

Hexagonal or circular pellets of these precursors were produced by uniaxial pressing of the precursor powder within hardened steel dies inside the argon-atmosphere glove box. The hexagonal pellets possessed edge-to-edge widths of $\approx$6.6 mm and thicknesses of 2-3 mm. The circular pellets were $\approx$10 mm in diameter and 2-3 mm thick. Because the Ba-Al-Al_2O_3-SiO_2 precursors consisted of $\approx$49.7 vol% ductile metal (i.e., Ba+Al), these precursors could be pressed to a relatively high density. For example, an Archimedes measurement conducted on the precursor pellet shown in Fig. 24a yielded a theoretical density of 94.1%.

Tapes were also prepared by packing and vacuum sealing a given powder batch into a fugitive silver tube. The tube was rolled at room temperature into a tape with a thickness of $\approx$500 μm (see discussion on page 11 for additional details of the rolling procedure). After every 50% reduction in the tape thickness, a vacuum annealing treatment was conducted at 300°C for 1 hour in order to avoid edge cracking of the silver sheathing.

b) Oxidation Processing

Several Ba-Al-Al_2O_3-SiO_2 pellets were placed on a bed of alumina powder within an alumina combustion boat. The pellet-bearing boat was then sealed inside a quartz tube within the argon atmosphere of the glovebox. The quartz tube contained valved inlet and outlet ports to allow for purging (just prior to oxidation) with flowing oxygen. The quartz tube was removed from the glove box and placed inside a horizontal tube furnace. The quartz tube was then purged with purified, flowing oxygen. The furnace was heated at a rate of 1°C/min from room temperature to 300°C and held at this temperature for 24 hours. The quartz tube was then removed from the furnace and allowed to cool, whereupon it was evacuated and transferred inside the argon-atmosphere glove box. One sample was removed from the quartz tube for x-ray diffraction analysis. The quartz tube was then re-sealed within the glove box and placed back into the

III. Results and Discussion (cont.)

A. Synthesis of Monolithic Celsian (cont.)

2. Metal/Oxide Precursors (cont.)

b) Oxidation Processing (cont.)

furnace and the remaining samples were exposed to a second heat treatment at a higher temperature (e.g., 500°C or 650°C) in flowing oxygen (heating and cooling were conducted in a similar manner as for the 300°C heat treatment). After the second treatment, a second sample was removed for x-ray diffraction analysis. This sequence was repeated with further consecutive heat treatments of up to 1200°C. Additional heat treatments up to 1650°C were conducted in ambient air in a box furnace (the box furnace heating rate was ≈30°C/min). Schema of the thermal treatments used are shown in Figs. 16a and 16b. As with Ba-Al-Si precursors, prolonged annealing times (10-96 hours) were used to allow for the formation of relatively coarse phases at a given temperature, for subsequent evaluation by electron microscopy.

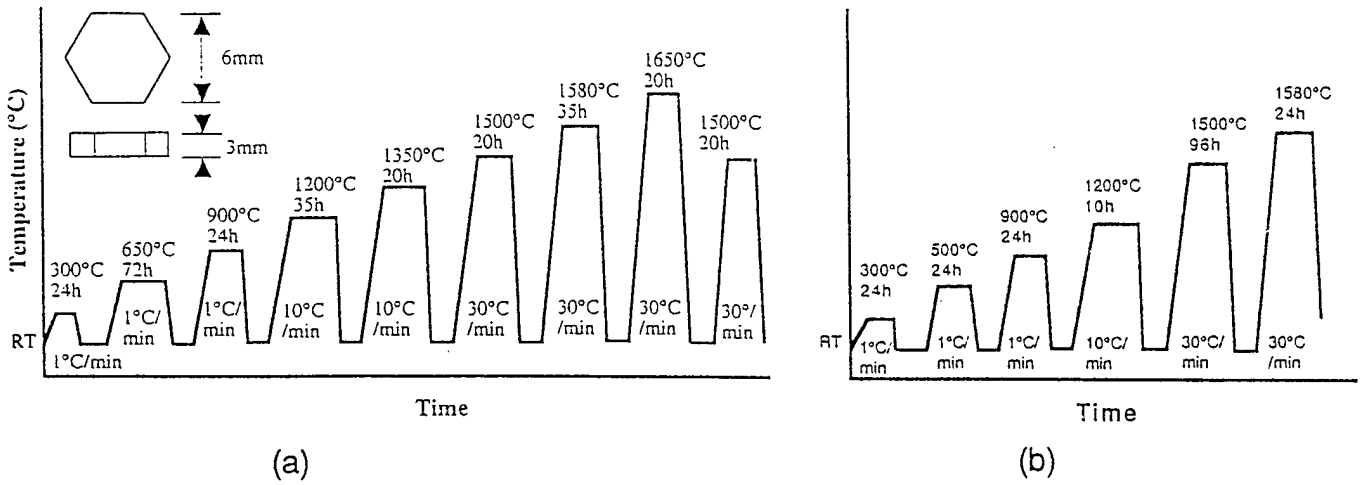

Figure 16. Heat treatment cycles used to oxidize and transform the Ba-Al-Al_2O_3-SiO_2 precursors. The schematic inset in (a) reveals the geometry of the hexagonal pellet specimens.

c) Phase and Microstructural Evolution

The phase and microstructural evaluation of Ba-Al-Al_2O_3-SiO_2 pellet specimens exposed to the heat treatment cycle shown in Fig. 16a were examined with XRD analyses and electron microscopy.

After exposure to O_2(g) at a peak temperature of 300°C:

XRD spectra obtained from air-quenched specimens after thermal treatment in flowing oxygen at peak temperatures of 300-1650°C are shown in Fig. 17. After exposure to flowing oxygen for 24 hours at 300°C, predominant diffraction peaks for Ba_2SiO_4 and SiO_2 (cristobalite) were detected. Peaks of relatively low intensity were also observed for Al and possibly for $BaAl_2O_4$[9]. Major diffraction peaks for BaO_2 were absent, although a small amount of $BaCO_3$ was detected. The presence of some $BaCO_3$ was attributed to reaction (perhaps of BaO_2) with CO_2 present in ambient air during transfer of the specimens to the x-ray diffractometer (note: the flowing oxygen used to oxidize the specimens was scrubbed of carbon dioxide and water vapor with an ascarite/drierite column).

---

9 While the strongest diffraction peak for $BaAl_2O_4$ overlaps a peak for Ba_2SiO_4 (e.g., the peak near 2θ = 28.3°), a minor non-overlapped peak for $BaAl_2O_4$ (near 2θ = 34.2°) was detected.

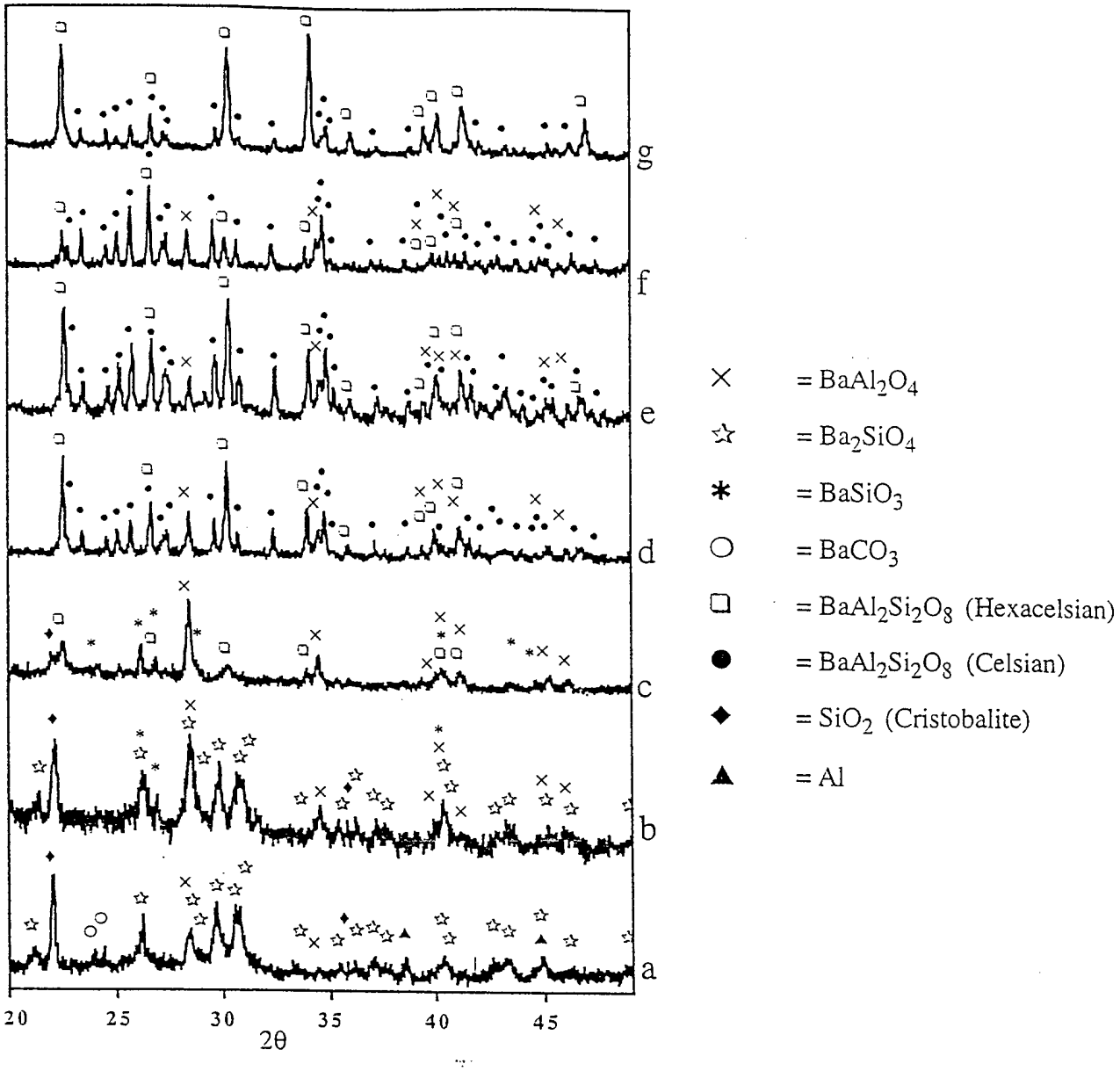

Figure 17. XRD spectra taken from the powderized Ba-Al-Al_2O_3-SiO_2 pellet specimens that were quenched after heat treatment at: a) 300°C for 24 hours, b) 650°C for 72 hours, c) 900°C for 24 hours, d) 1200°C for 35 hours, e) 1350°C for 20 hours, f) 1580°C for 35 hours, and g) 1650°C for 20 hours, followed by 1500°C for 20 hours (using the heat treatment cycle shown in Fig. 16a). Heat treatments at ≤1200°C and at ≥1350°C were conducted in flowing O_2(g) and ambient air, respectively.

A backscattered electron image and associated x-ray dot maps of a specimen quenched from a peak temperature of 300°C are shown in Figs. 18a-d. A bright, aluminum-depleted phase (labeled B_2S) can be seen, along with a gray, silicon-depleted matrix phase (labeled BA). Dark particles enriched in either aluminum (labeled A) or silicon (labeled S) can also be seen. Several A and S particles were of sufficiently large size as to allow for unambiguous EDX confirmation that such particles were aluminum or silica. Unfortunately, the presence of fine, closely-spaced aluminum and silica particles mixed in with the BA and B_2S phases inhibited unambiguous, quantitative EDX confirmation of the compositions of the BA and B_2S phases (TEM analyses are in progress). Nonetheless, reference to the XRD pattern in Fig. 17 leads to the tentative conclusion that the BA and B_2S phases were $BaAl_2O_4$ and Ba_2SiO_4, respectively.

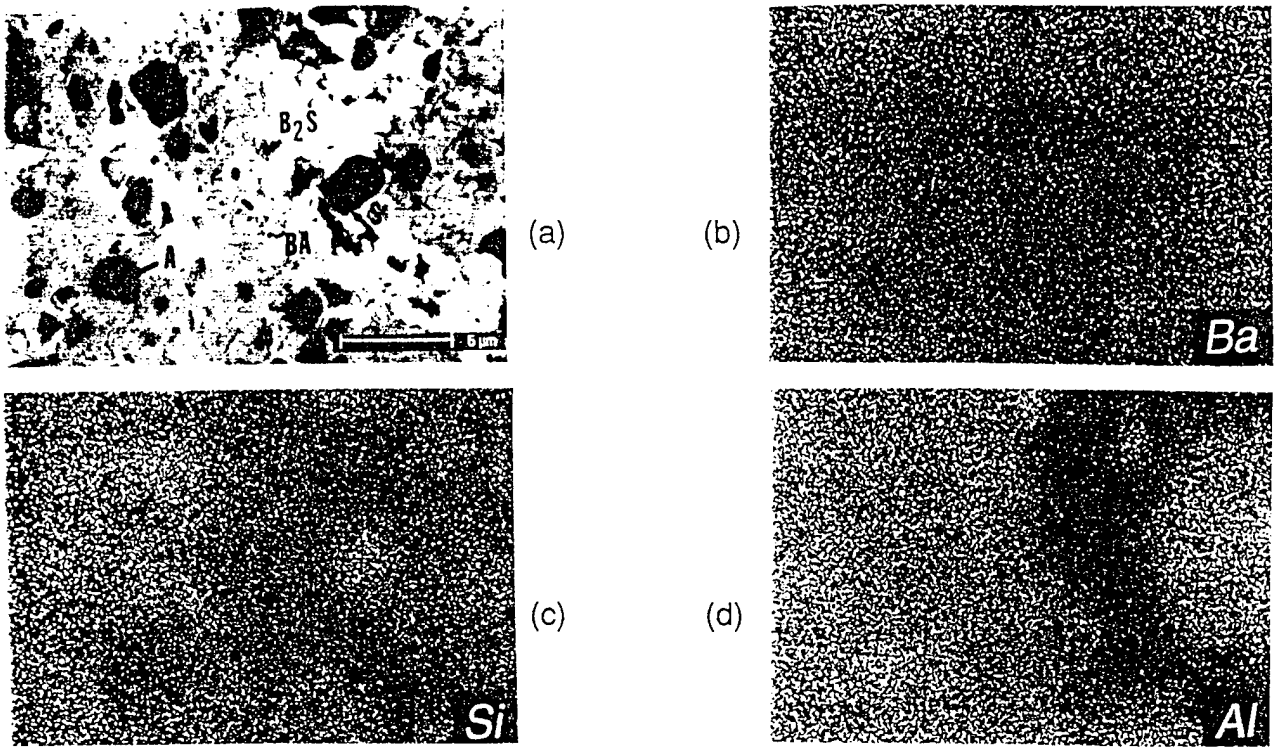

Figure 18. (a) Backscattered electron image and (b)-(d) associated x-ray dot maps of a polished cross-section of a quenched Ba-Al-Al_2O_3-SiO_2 pellet specimen that had been exposed to flowing oxygen for 24 hours at 300°C. (A = aluminum, S = SiO_2, BA = $BaAl_2O_4$ (deduced from XRD analyses), B_2S = Ba_2SiO_4 (deduced from XRD analyses))

After exposure to O_2(g) at a peak temperatures of 650°C and 900°C:

After 72 hours at 650°C, the aluminum peaks had vanished and the peaks for $BaAl_2O_4$ increased in relative intensity. Diffraction peaks for Ba_2SiO_4 and SiO_2 were still present. A small amount of $BaSiO_3$ was also detected.

The diffraction peaks for the $BaAl_2O_4$ phase were most dominant after 24 hours at 900°C. The diffraction peaks for $BaSiO_3$ became more distinct at the expense of peaks for Ba_2SiO_4 and SiO_2, which had vanished and significantly decreased in intensity, respectively. Hexacelsian had also begun to form at ≤900°C.

After exposure to O_2(g) at peak temperatures of 1200-1500°C:

After 35 hours at 1200°C, an appreciable amount of hexacelsian had transformed into celsian. Diffraction peaks for cristobalite had vanished, although peaks for residual $BaAl_2O_4$ remained after this heat treatment. Additional heat treatments at 1350°C and 1500°C resulted in an increase in the intensities of peaks for celsian at the expense of peaks for hexacelsian. Residual $BaAl_2O_4$ was retained after firing at a peak temperature of 1500°C for 20 hours. Nonetheless, no distinct, unambiguous diffraction peaks for binary barium silicates could be detected in the specimens quenched from 1200-1500°C.

Backscattered electron images and associated x-ray dot maps of two cross-sectional areas of a specimen quenched after 35 hours at 1200°C are shown in Figs. 19a-d and 20a-d. In Fig.

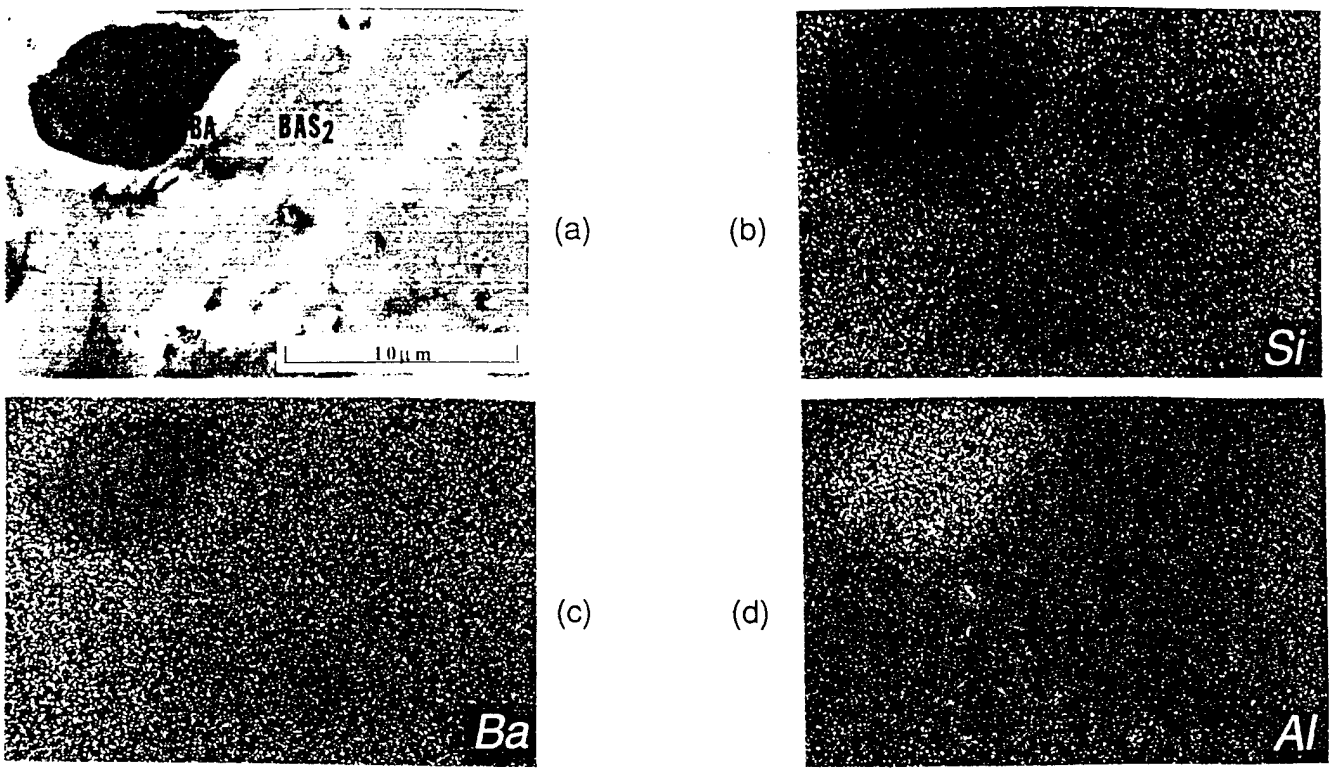

Figure 19. (a) Backscattered electron image and (b)-(d) associated x-ray dot maps of a polished cross-section of a quenched Ba-Al-Al_2O_3-SiO_2 pellet specimen that had been exposed to flowing oxygen for 35 hours at a peak temperature of 1200°C (using the heat treatment cycle in Fig. 16a). (AO = Al_2O_3, BA = $BaAl_2O_4$ (deduced from XRD analyses), BAS_2 = BaO-Al_2O_3-$2SiO_2$)

19a, an aluminum-rich particle (labeled AO) can be detected within a gray matrix phase (labeled BAS_2). The composition of the gray matrix phase was 41.0 wt% BaO, 26.7 wt% Al_2O_3, and 32.3 wt% SiO_2, which is similar to that for $BaAl_2Si_2O_8$ (40.8 wt% BaO, 27.2 wt% Al_2O_3, 32.0 wt% SiO_2). EDX analyses revealed that the aluminum-rich particle consisted of aluminum oxide. A thin, bright coating (1-2 μm thick) was observed to surround the alumina particle. Barium, aluminum, and silicon dot maps indicated that the coating contained barium and aluminum and was depleted in silicon. Indeed, the brightness of the coating relative to the gray matrix indicates that the coating was barium rich with respect to $BaAl_2Si_2O_8$. Quantitative EDX analysis (of a thicker coating around another alumina particle not shown) yielded a composition of 61.3 wt% BaO, 33.9 wt% Al_2O_3, and 4.8 wt% SiO_2, which is consistent with $BaAl_2O_4$ (60.1 wt% BaO, 39.9 wt% Al_2O_3 - some overlap of the beam interaction zone with the matrix may be responsible for the silica detected in the EDX analysis). Hence, both XRD and EDX analyses confirmed the presence of $BaAl_2O_4$ and $BaAl_2Si_2O_8$ in specimens quenched from 1200°C.

In Fig. 20a, fine, bright particles (labeled BS) depleted of aluminum are observed in a gray matrix. EDX analyses confirmed that the matrix phase was $BaAl_2Si_2O_8$. While the bright particles shown in Fig. 20a were too fine to allow for unambiguous EDX analyses, analysis of a larger particle of similar brightness yielded a composition of 69.7 wt% BaO, 5.7 wt% Al_2O_3, and 24.6 wt% SiO_2, which is similar to that expected for $BaSiO_3$ (71.8 wt% BaO, 28.2 wt% SiO_2).. However, $BaSiO_3$ was not evident in the XRD analyses of this specimen. Either the volume fraction of these particles may not have been sufficient to allow for detection by XRD or these particles may have consisted of an amorphous silicate. Further TEM analyses is underway to

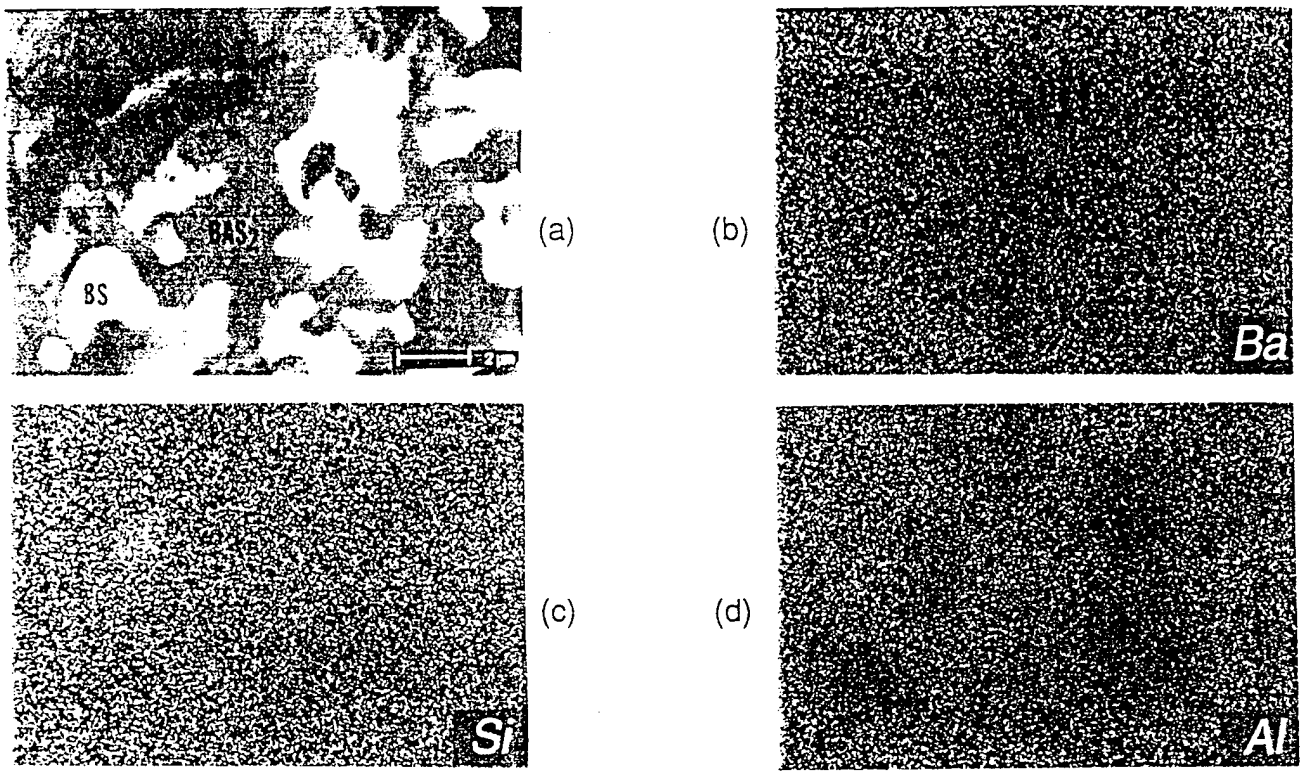

Figure 20. (a) Backscattered electron image and (b)-(d) associated x-ray dot maps of a polished cross-section of a quenched Ba-Al-Al_2O_3-SiO_2 pellet specimen that had been exposed to flowing oxygen for 35 hours at a peak temperature of 1200°C (using the heat treatment cycle in Fig. 16a). (BS = $BaSiO_3$, BAS_2 = BaO-Al_2O_3-$2SiO_2$)

identify these particles. Nonetheless, EDX and XRD analyses were consistent in detecting the presence of both $BaAl_2Si_2O_8$ and residual $BaAl_2O_4$ in the specimen quenched from 1200°C.

After exposure to O_2(g) at a peak temperature of 1650°C, followed by 1500°C:

In order to allow for more complete consumption of residual $BaAl_2O_4$, pellet specimens were further annealed for 20 hours at 1650°C. This thermal treatment was followed by 20 hours at 1500°C, in order to reform monoclinic celsian from hexacelsian produced at 1650°C (monoclinic celsian becomes thermodynamically unstable above ≈1590°C [21, 22]). After such heat treatment, XRD analysis revealed that $BaAl_2O_4$ had been completely consumed. The most dominant diffraction peaks were associated with hexacelsian, however, as only partial reconversion back to monoclinic celsian had occurred within 20 hours at 1500°C. A backscattered electron image and associated dot maps of such a specimen are shown in Figs. 21a-d. The x-ray maps revealed a relatively uniform distribution of barium, aluminum, and silicon. Quantitative EDX analyses of the gray matrix phase shown in Fig. 21a yielded a composition of 38.1 wt% BaO, 29.1 wt% Al_2O_3, and 32.8 wt% SiO_2, which is consistent with $BaAl_2Si_2O_8$ (40.8 wt% BaO, 27.2 wt% Al_2O_3, and 32.0 wt% SiO_2).

The consumption of $BaAl_2O_4$ at 1500-1650°C indicated that a source of silica was present that could not be detected in the XRD patterns. One possible source is an amorphous silicate (perhaps the fine BS particles in Fig. 20a). In the work discussed above on the transformation of Ba-Al-Si precursors, TEM analyses revealed that an amorphous silicate phase was produced at 1200°C. This silicate possessed a composition close to that expected for an oxide liquid that

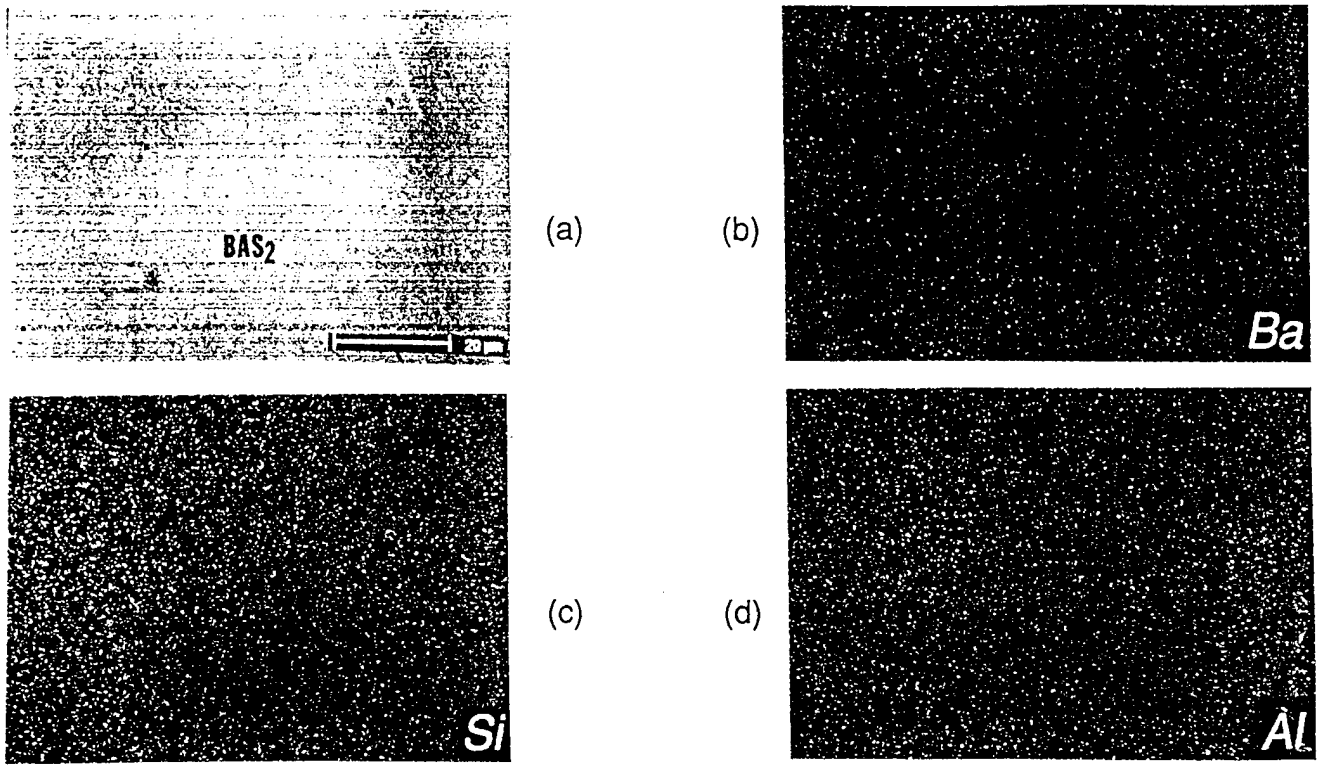

Figure 21. (a) Backscattered electron image and (b)-(d) associated x-ray dot maps of a polished cross-section of a quenched Ba-Al-Al_2O_3-SiO_2 pellet specimen that had been exposed to ambient air for 20 hours at a peak temperature of 1650°C, followed by 20 hours at 1500°C (using the heat treatment cycle in Fig. 16a). (BAS_2 = $BaO{\cdot}Al_2O_3{\cdot}2SiO_2$)

can be produced in the BaO-Al_2O_3-SiO_2 system at 1200°C [21, 22]. It is possible that such a silicate was also produced in the Ba-Al-Al_2O_3-SiO_2 specimens during exposure to temperatures ≥1200°C. TEM analyses are underway to determine if such a liquid was indeed present in these partially-transformed metal-oxide specimens.

A summary of the phases detected at various stages of transformation of the Ba-Al-Al_2O_3-SiO_2 precursors to celsian is presented in Table 4 below. Comparison of the data in Tables 2 and 4 reveals some similarities and differences in the intermediate reaction products preceding $BaAl_2Si_2O_8$ from Ba-Al-Si and Ba-Al-Al_2O_3-SiO_2 precursors. For both types of precursors, Ba_2SiO_4 was produced within 20-24 hours at 300°C. In other words, the formation of Ba_2SiO_4 by the reaction of oxidized barium with a silicon source takes place at ≤300°C whether the silicon source is Si or SiO_2. A Ba-Si-O glass phase was detected between oxidized barium and Si in the TEM image shown in Fig. 9d. Mass transport across this glassy phase or across crystalline Ba_2SiO_4 may be the rate-limiting process for the formation of Ba_2SiO_4 in Ba-Al-Si precursors at ≤400°C. If so, and if a similar amorphous phase is present between oxidized barium and Ba_2SiO_4 present in Ba-Al-Al_2O_3-SiO_2 precursors at ≤400°C, then the rate of formation of Ba_2SiO_4 may not be strongly dependent on the Si-bearing phase present in the starting precursor. Further TEM work is needed to reveal the morphology of the interface between BaO_2 and SiO_2 in Ba-Al-Al_2O_3-SiO_2 precursors at ≤400°C.

While Ba-Al-O glass was detected by TEM analyses at 400°C in the Ba-Al-Si precursors, only for the Ba-Al-Al_2O_3-SiO_2 precursors was crystalline $BaAl_2O_4$ detected by XRD or

III. Results and Discussion (cont.)

A. Synthesis of Monolithic Celsian (cont.)

2. Metal/Oxide Precursors (cont.)

c) Phase and Microstructural Evolution (cont.)

SEM/EPMA at ≥300°C. It appears that the rate of formation of $BaAl_2O_4$ was strongly enhanced by either the presence of some Al_2O_3 in the starting precursor or by the absence of elemental silicon. If the formation of $BaAl_2O_4$ was enhanced by the presence of Al_2O_3, then the formation of $BaAl_2O_4$ in the Ba-Al-Si precursors should have lagged behind the oxidation of aluminum. Indeed, if BaO_2 is completely consumed by reaction with silicon (to form Ba_2SiO_4) before appreciable reaction can take place between BaO_2 and oxidized aluminum (as appears to have happened during oxidation of the Ba-Al-Si precursors), the $BaAl_2O_4$ may be bypassed as an intermediate reaction product. The presence of some Al_2O_3 in the Ba-Al-Al_2O_3-SiO_2 precursors may have allowed for the formation of some $BaAl_2O_4$ prior to complete consumption of BaO_2. Additional work is required to evaluate the role of Al_2O_3 on the rate of formation of $BaAl_2O_4$.

Table 4. Phase Evolution to Celsian from Ba-Al-Al_2O_3-SiO_2 Precursors

Temperature/Time/Cycle			Phases Detected	Detection Method*
300°C	24 hours	3†	Ba_2SiO_4	XRD
			SiO_2	XRD, EDX
			Al	XRD, EDX
			$BaAl_2O_4$	XRD
			$BaCO_3$+	XRD
650°C	72 hours	3	Ba_2SiO_4	XRD
			SiO_2	XRD
			$BaAl_2O_4$	XRD
			$BaSiO_3$	XRD
900°C	24 hours	3	$BaAl_2O_4$	XRD
			SiO_2	XRD
			$BaSiO_3$	XRD
			hex-$BaAl_2Si_2O_8$	XRD
1200°C	35 hours	3	$BaAl_2O_4$	XRD
			hex-$BaAl_2Si_2O_8$	XRD, EDX#
			mono-$BaAl_2Si_2O_8$	XRD, EDX#
			Al_2O_3	EDX
1350°C	20 hours	3	$BaAl_2O_4$	XRD
			hex-$BaAl_2Si_2O_8$	XRD
			mono-$BaAl_2Si_2O_8$	XRD
1500°C	20 hours	3	$BaAl_2O_4$	XRD
			hex-$BaAl_2Si_2O_8$	XRD
			mono-$BaAl_2Si_2O_8$	XRD
1650°C	20 hours	3	hex-$BaAl_2Si_2O_8$	XRD, EDX#
then 1500°C	20 hours		mono-$BaAl_2Si_2O_8$	XRD, EDX#

* EDX= energy-dispersive x-ray analysis via SEM

‡ Presumed to have been BaO_2 prior to reaction with CO_2(g) in ambient air.

† Cycle 3 refers to the heat treatment cycle shown in Fig. 16a.

\# While EDX analyses can not distinguish between hexacelsian and monoclinic celsian, the presence of $BaAl_2Si_2O_8$ was confirmed.

III. Results and Discussion (cont.)

A. Synthesis of Monolithic Celsian (cont.)

2. Metal/Oxide Precursors (cont.)

c) Phase and Microstructural Evolution (cont.)

Hexacelsian preceded the formation of monoclinic celsian with both types of precursors. Several authors have reported that substitution of some of the barium with strontium in precursors to celsian dramatically enhances the rate of formation of monoclinic celsian [69, 72]. Hence, in order to enhance the rate of transformation of hexacelsian to monoclinic, half of the barium was replaced in some of the metal/oxide specimens by strontium. The consequences of partial substitution of barium with magnesium have also been examined. The results of such experiments are discussed in the following section.

d) Effects of Sr and Mg Doping

Pellets were prepared by uniaxial pressing of precursor powder with targeted Ba: Sr or Mg: Al: Al_2O_3: SiO_2 molar ratios of 0.50: 0.50: 1.68: 0.16: 2.00. XRD patterns of the Ba-Sr-Al-Al_2O_3-SiO_2 and Ba-Al-Al_2O_3-SiO_2 specimens after heat treatments at peak temperatures of 1200°C are presented in Figs. 22a and 22b, respectively. The strontium-doped sample was exposed for a shorter time at ≤1200°C than the strontium-free sample (i.e., the heat treatment cycle of Fig. 16b was used to oxidize the Sr-bearing sample, whereas the cycle of Fig. 16a was used for the Sr-free sample). As discussed above, the XRD pattern of the strontium-free sample revealed peaks for $BaAl_2O_4$, hexacelsian, and monoclinic celsian. However, after 10 hours at 1200°C, only peaks for monoclinic celsian were detected in the strontium-doped pellets. Clearly, the rate of conversion to celsian in these strontium-bearing precursors was faster than for strontium-free precursors. This is consistent with prior work of other authors who found that partial substitution of strontium for barium in mixed salt or glass precursors enhanced the formation of monoclinic celsian [69, 72].

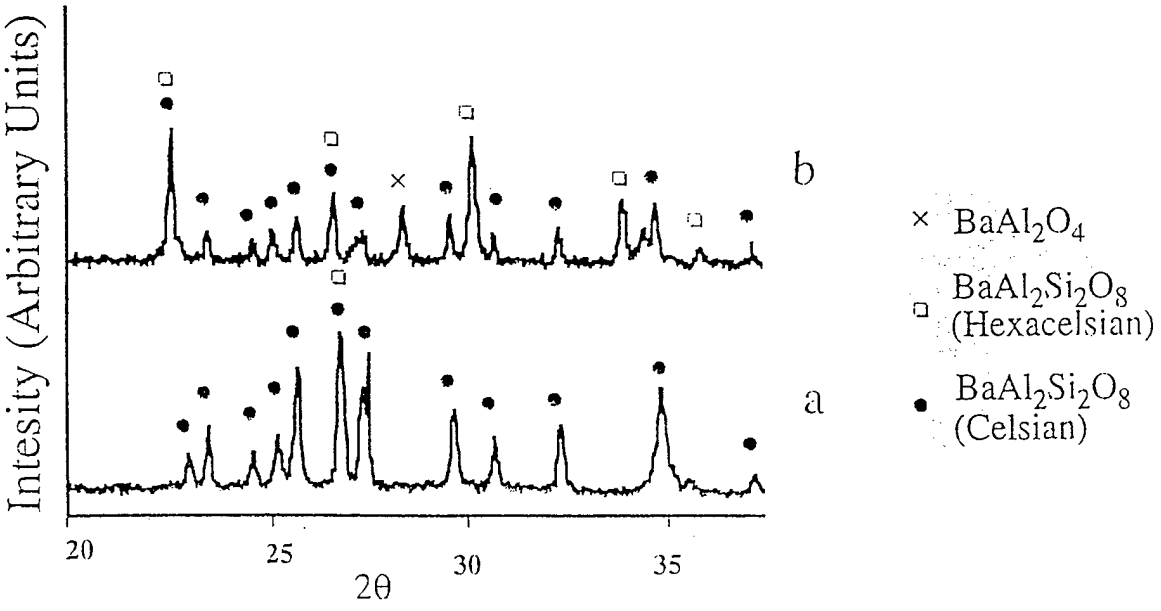

Figure 22. XRD spectra obtained from (a) a powderized Ba-Sr-Al-Al_2O_3-SiO_2 pellet specimen that had been exposed to a peak temperature of 1200°C for 10 hours (via the heat treatment cycle shown in Fig. 16b) and (b) Ba-Al-Al_2O_3-SiO_2 pellet specimens that had been exposed to a peak temperature of 1200°C for 35 hours (via the heat treatment cycle shown in Fig. 16a)

III. Results and Discussion (cont.)

A. Synthesis of Monolithic Celsian (cont.)

2. Metal/Oxide Precursors (cont.)

d) Effects of Sr and Mg Doping (cont.)

An XRD pattern of a magnesium-doped specimen exposed for 10 hours at 1200°C is shown in Fig. 23b below (the heat treatment cycle of Fig. 16b was used). Dominant peaks for monoclinic celsian and osumilite, $BaMg_2Al_6Si_9O_{30}$, were detected. Three unidentified peaks (located at $2\theta \approx 29.9°$, 31.6°, 32.8°) were also detected[10]. Whereas residual $BaAl_2O_4$ was detected in this specimen, diffraction peaks for hexacelsian peaks were absent. While the XRD pattern in Fig. 23b reveals that the synthesis of osumilite by the SMP method is possible, strontium substitution for barium appears to be a more effective means of producing pure, monoclinic celsian than magnesium substitution.

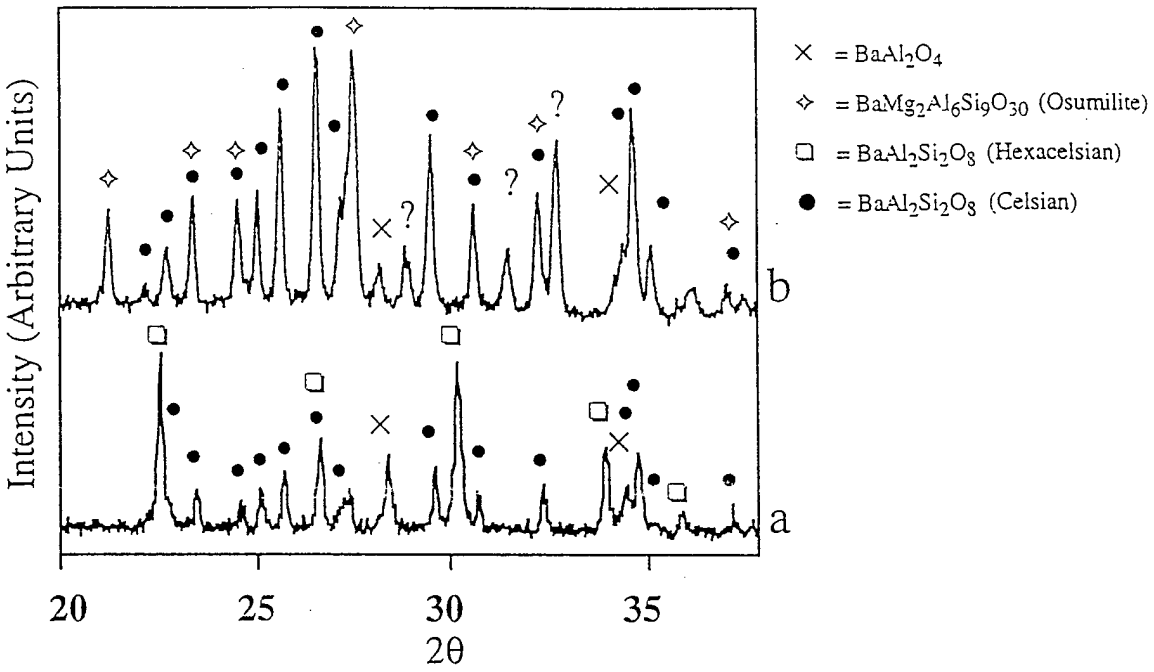

Figure 23. XRD spectra obtained from (a) a Ba-Al-Al_2O_3-SiO_2 pellet specimens that had been exposed to a peak temperature of 1200°C for 35 hours (via the heat treatment cycle shown in Fig. 16a) and (b) a powderized Ba-Mg-Al-Al_2O_3-SiO_2 pellet specimen that had been exposed to a peak temperature of 1200°C for 10 hours (via the heat treatment cycle shown in Fig. 16b).

e) Near Net-Shaped Celsian Bodies

Net reactions to celsian from Ba-Al-Al_2O_3-SiO_2 or Ba-Sr-Al-Al_2O_3-SiO_2 precursors are shown below.

Precursor		Product(s)	
1.0 Ba + 1.68 Al + 0.16 α-Al_2O_3 + 2 SiO_2(cristobalite)	heat ===> + oxygen	1.0 $BaAl_2Si_2O_8$	(5)
0.50 Ba + 0.50 Sr + 1.68 Al + 0.16 α-Al_2O_3 + 2 SiO_2(cristobalite)	heat ===> + oxygen	1.0 $(Ba_{0.5}Sr_{0.5})Al_2Si_2O_8$	(6)

[10] JCPDS card files for magnesium-bearing compounds such as $MgAl_2O_4$, $MgSiO_3$, Mg_2SiO_4, $Mg_2Al_4SiO_{10}$, $Mg_2AlSi_5O_{18}$, $BaMg_2Si_2O_7$, $BaMgSiO_4$, $Ba_3MgSi_2O_8$, and $Ba_2MgSi_2O_7$ did not provide definitive matches to these unidentified peaks.

III. Results and Discussion (cont.)

A. Synthesis of Monolithic Celsian (cont.)

2. Metal/Oxide Precursors (cont.)

e) Near Net-Shaped Celsian Bodies (cont.)

The volume changes associated with net reactions (5) and (6) were calculated to be ≈+0.1%, and -0.2%, respectively (% vol. change = $100 \cdot [V_{product} - V_{precursor}]/V_{precursor}$). In other words, if such dense precursors can be completely transformed into dense $BaAl_2Si_2O_8$ or $(Ba_{0.5}Sr_{0.5})Al_2Si_2O_8$, then the observed volume change should be minimal. If such transformation occurs uniformly throughout a bulk, intimately-mixed precursor, then the resulting change in a given specimen dimension should also be quite small.

Optical images of a Ba-Sr-Al-Al_2O_3-SiO_2 hexagonal precursor pellet before oxidation and after complete transformation into $(Ba_{0.5}Sr_{0.5})Al_2Si_2O_8$ are shown in Figs. 24a and 24b, respectively (a peak firing temperature of 1580°C for 24 hours was used to transform the pellet via the heat treatment cycle of Fig. 16a). The average edge-to-edge dimensions of the hexagonal pellets shown in Figs. 24a and 24b were 6.58 and 6.65 mm, respectively, which corresponds to a relative dimensional change of only 1%. XRD data confirmed that the pellet was composed of only monoclinic celsian. Archimedes density measurements indicated that the transformed pellet shown in Fig. 24b possessed a density that was 98.5% of the theoretical density of $(Ba_{0.5}Sr_{0.5})Al_2Si_2O_8$. Such a result demonstrates the feasibility of fabricating dense, near net-shaped celsian by the SMP method.

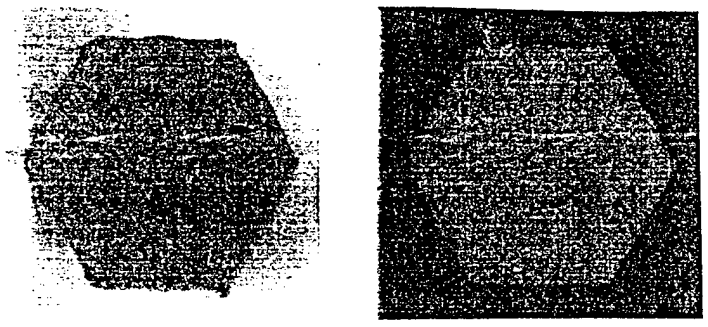

(a) (b)

Figure 24. Optical photographs of a Ba-Sr-Al-Al_2O_3-SiO_2 precursor pellet (a) before and (b) after heat treatment at a peak temperature of 1580°C for 24 hours (using the heat treatment cycle shown in Fig. 16a). The pellet shown in b) has been completely transformed into $(Ba_{0.5}Sr_{0.5})Al_2Si_2O_8$..

B. Syntheses of Celsian Composites

The syntheses of three types of celsian-matrix composites have been examined to date: celsian-zirconia, celsian-alumina, and celsian-silicon nitride. The results of this work are discussed below.

1. Celsian/Zirconia

A potentially-attractive feature of celsian-zirconia composites is enhanced fracture toughness resulting from the tetragonal-to-monoclinic transformation of zirconia particles, in a manner analogous to other zirconia-toughened ceramics [23, 73-77]. Indeed, celsian-zirconia

composites containing 20 mol% zirconia have exhibited higher indentation hardness than pure celsian [23]. Zirconia additions to celsian have also been found to enhance densification [23].

a) Precursor Preparation, Oxidation Processing

Ba-Si-Al_2O_3-SiO_2-ZrO_2 precursor mixtures were prepared by mechanical alloying. The targeted molar Ba: Si: Al_2O_3: SiO_2: ZrO_2 ratio of this precursor was 1.00: 0.90: 1.00: 1.10: 0.91. The only ductile metal present in this phase assemblage was barium, which consisted of only 32.1 vol% of the precursor. Consequently, uniaxial pressing yielded pellets that were ≤88% of the theoretical density. In order to partially compensate for sintering shrinkage resulting from the removal of the porosity in the starting precursor, the molar ratios of species in these precursors were chosen such that the reaction-induced volume change would be +9.4% (that is, the molar volume of this precursor was about 9.4% lower than the calculated molar volume of the celsian-zirconia composite that would be produced upon complete transformation, ignoring any solid solubility of zirconia in celsian).

The Ba, Si, Al_2O_3, and SiO_2 starting components are the same as those listed in Table 3 (page 26). The zirconia was obtained (Johnson-Matthey, Ward Hill, MA) as powder with a purity of 99.9% and an average particle size of 5 μm. A 3.5 g batch of this powder was sealed within a yttria-stabilized zirconia vial (in the argon-atmosphere glove box) along with 2 yttria-stabilized zirconia balls and 30 mL of hexane. High-energy vibratory milling was conducted for 7 hours. After filtration and evaporation of the hexane, the resulting powder mixture was uniaxially pressed into pellets with a diameter of 10 mm and a thickness of ≈3 mm.

The Ba-Al_2O_3-Si-SiO_2-ZrO_2 precursors to celsian-zirconia were first oxidized in pure, flowing oxygen with successive 24 hours anneals each at 300°C, 500°C, and 900°C. The pellets were then heated in air at 1200°C for 26 hours, followed by 1350°C for 20 hours and then 1580°C for 20 hours.

b) Transformation to Net-Shaped Celsian-Zirconia Composites

X-ray diffraction patterns obtained from powderized pellets of the Ba-Al_2O_3-Si-SiO_2-ZrO_2 precursor after firing at peak temperatures of 1200°C and 1580°C are presented in Figs. 25a and b, respectively. In both patterns, peaks for monoclinic celsian and monoclinic zirconia were detected. Based on the intensities of zirconia and celsian peaks, it appears that the relative amount of zirconia detected after the 1580°C heat treatment was greater than after the 1200°C heat treatment. Further work is underway to determine whether this apparent increase in the amount of the zirconia phase was a result of the exsolution at 1580°C of some zirconia that, at 1200°C, had been dissolved in a solid solution with monoclinic celsian. (Debsikdar and Sowemimo reported that 10 mole% or more zirconia could be dissolved in solid solution with hexacelsian at 1050°C [23].) Comparison of the x-ray patterns in Figs. 25a, 17, and 12 also suggests that the zirconia in these specimens may have enhanced the formation of monoclinic celsian relative to hexacelsian at 1200°C. A secondary electron image and a zirconium x-ray dot map of a fracture section of a celsian-zirconia composite produced after firing at a peak temperature of 1580°C for 20 hours are shown in Fig. 26. The zirconium x-ray map reveals the free zirconia particles present in the celsian matrix. The data shown in Figs. 25 and 26 demonstrate the feasibility of synthesizing composites of monoclinic celsian and zirconia at 1200-1580°C from Ba-Al_2O_3-Si-SiO_2-ZrO_2 precursors. Measurements of the diameters of circular pellets before and after complete transformation revealed small changes in dimensions (1-3%), thereby confirming that celsian-zirconia composites could be produced from Ba-Al_2O_3-Si-SiO_2-ZrO_2 with a retention of shape.

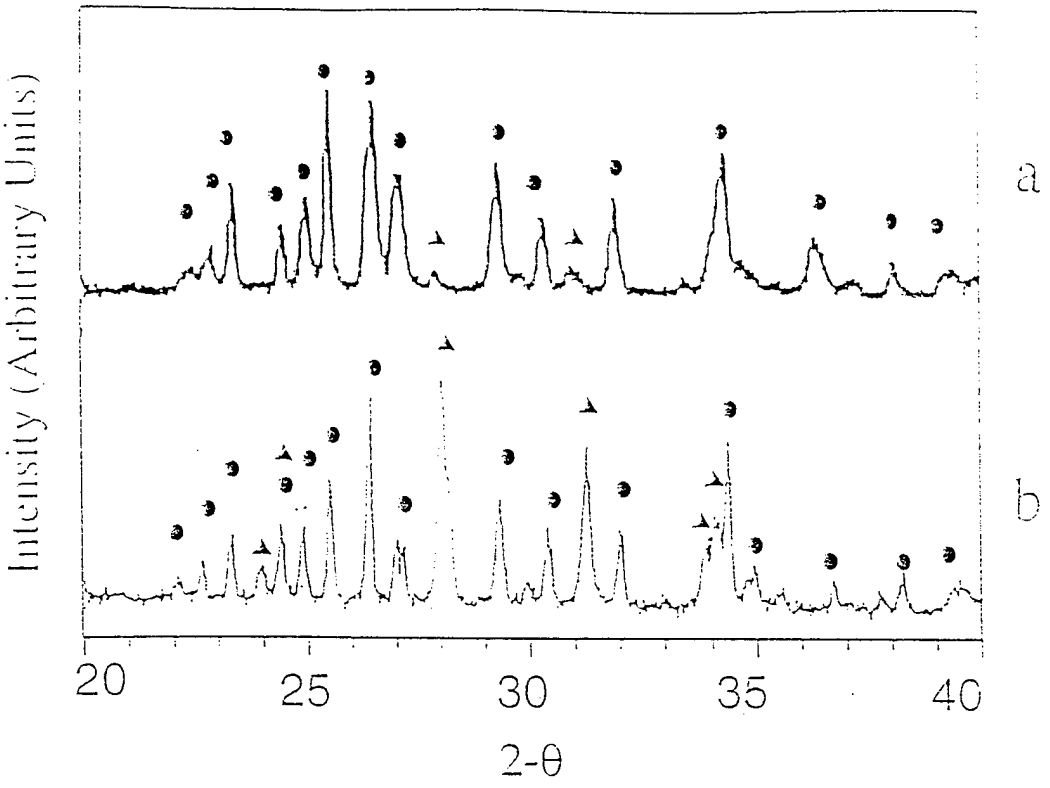

Figure 25. XRD spectra obtained from a Ba-Al_2O_3-Si-SiO_2-ZrO_2 pellet specimens that had been exposed to a peak temperature of (a) 1200°C for 26 hours and (b) 1580°C for 20 hours. Filled circles and triangles represent monoclinic celsian and monoclinic zirconia, respectively.

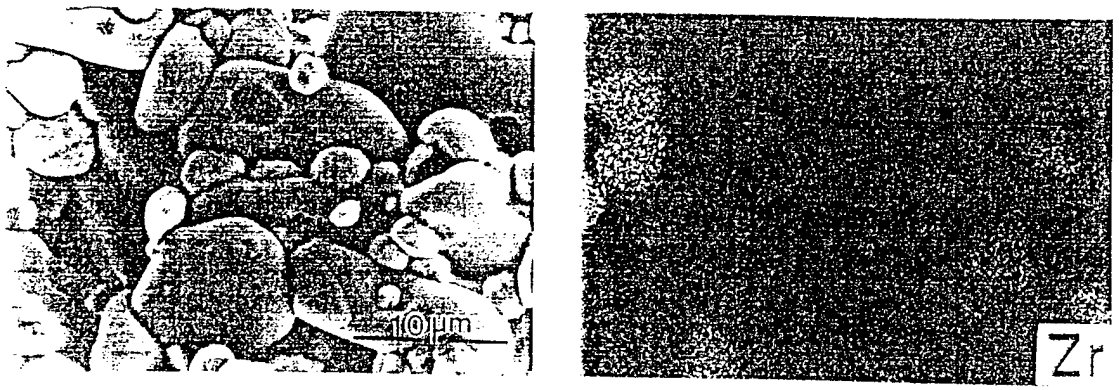

(a) (b)

Figure 26. (a) Secondary electron image and (b) zirconium x-ray dot map of a fracture section of a Ba-Al_2O_3-Si-SiO_2-ZrO_2 pellet specimen that had been exposed to a peak temperature of 1580°C for 20 hours.

III. Results and Discussion (cont.)

A. Synthesis of Celsian Composites (cont.)

2. Altex™ Fiber-bearing Composites

a) Precursor Preparation, Oxidation Processing

A discontinuous-fiber-reinforced, celsian-matrix composite has also been produced by a method similar to that shown in Fig. 3. In this case, Altex™ aluminosilicate fibers (85% Al_2O_3, 15% SiO_2, ave. diameter of 15 μm)[11] were cut into 1 cm lengths and then blended with Ba-Si-Al_2O_3-SiO_2 precursor powder. The fiber content in the mixture was 10 vol%. In this case, the Ba-Si-Al_2O_3-SiO_2 precursor powder possessed a Ba: Si: Al_2O_3: SiO_2 atomic ratio of 1.00: 0.50: 1.00: 1.50. Work discussed on page 16 indicated that one fourth (at% basis) of the silicon in Ba-Al-Si precursors could be oxidized by reaction with BaO_2 at 300-500°C to yield Ba_2SiO_4. Hence, it should be possible to completely oxidize a Ba-Si-Al_2O_3-SiO_2 precursor with a Ba:Si ratio of 2:1 at ≤500°C. By completely oxidizing the silicon at such a modest temperature, the formation of $BaAl_2Si_2O_8$ at higher temperatures would not be slowed by the time required for silicon oxidation (note: the XRD data in Fig. 7 indicated that residual silicon was present in Ba-Al-Si precursors after 10 hours at 1200°C). The precursor-fiber mixture was packed into a fugitive silver tube, which was evacuated and welded shut. The tube was compacted and rolled into a tape (for details of rolling, see the discussion on page 11). The heat treatment cycle shown in Figure 27 was used to transform the precursor tape into an Altex-fiber-reinforced, celsian-matrix composite.

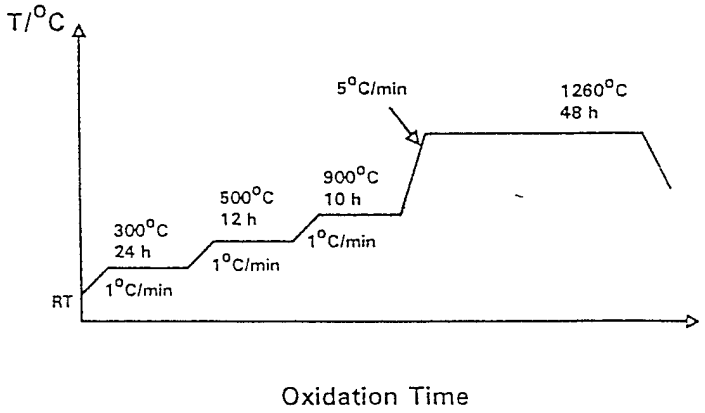

Figure 27. Heat treatment cycle used to transform an Altex™ fiber-bearing, Ba-Si-Al_2O_3-SiO_2 precursor into a discontinuous-Altex fiber-reinforced celsian-bearing composite.

b) Transformation to an Altex™ Fiber-bearing Composite

A secondary electron image of the composite produced by the heat treatment shown in Fig. 27 is shown in Fig. 28. The discontinuous fibers retained their round shape and approximate diameter after oxidation and transformation of the surrounding Ba-Si-Al_2O_3-SiO_2 precursor matrix (that is, appreciable consumption of the fibers during transformation of the matrix was not detected). No solid reaction products were detected by EPMA at the interface between the fibers and the $BaAl_2Si_2O_8$-bearing matrix, which was consistent with the fact that celsian and alumina are chemically compatible (i.e., a tie line exists between $BaAl_2Si_2O_8$ and Al_2O_3) [21, 22]. While mechanical testing of such discontinuously-reinforced composites remains to be conducted, along with further work to produce and test continuous-fiber-reinforced composites (i.e., by the method shown in Fig. 4), this preliminary work revealed that the synthesis of Altex-fiber-reinforced composites is possible by the method shown in Fig. 3.

---

11 Textron Specialty Materials, Lowell, MA

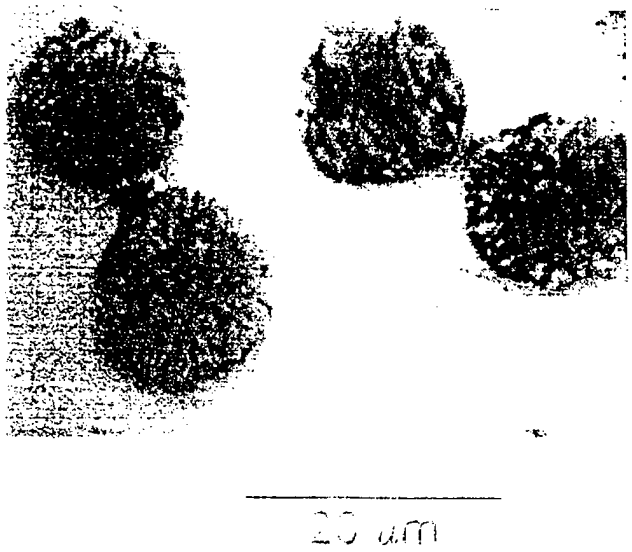

Figure 28. $BaAl_2Si_2O_8$-bearing, discontinuous Altex™ fiber composites produced by the SMP method shown schematically in Fig. 3.

3. Silicon Nitride-bearing Composites

Composites of celsian with silicon nitride have exhibited appreciably higher strengths and fracture toughness values than pure celsian [24, 26]. A particularly attractive feature of celsian-silicon nitride composites is the similarity in the (relatively low) thermal expansion coefficients of these compounds. Such a composite could be relatively resistant to damage from thermal cycling.

a) Precursor Preparation, Oxidation Processing

The barium, aluminum, alumina, and silica sources and purities were similar to those shown in Table 3 (page 26). Silicon nitride powder with a particle size of ≤40 μm and a purity of ≥98.7% was obtained from UBE industries. A precursor with a targeted Ba: Al: Al_2O_3: SiO_2: Si_3N_4 molar ratio of 1.00: 1.68: 0.16: 2.00: 2.28 (i.e., a near net-shape composition) was blended together. A 7 gram batch of the Ba-Al-Al_2O_3-SiO_2-Si_3N_4 mixture was milled in a zirconia vial for a period of only 80 minutes. After removal of the hexane, the silicon nitride-bearing powder mixture was packed and sealed (under vacuum) into a fugitive silver tube. The tube was compacted by rolling into a tape (see discussion of rolling conditions on page 11) with a thickness of ≈500 μm.

Silver-sheathed Ba-Al-Al_2O_3-SiO_2-Si_3N_4 precursor tapes were oxidized in pure, flowing oxygen in successive anneals of 24 hours each at 300°C, 500°C, and 900°C. The fugitive silver sheath was then removed after the 900°C heat treatment, and a subsequent treatment in pure, flowing nitrogen was conducted for 35 hours at 1200°C.

b) Reaction Products

The x-ray powder diffraction patterns obtained from a Ba-Al-Al_2O_3-SiO_2-Si_3N_4 precursor tape after heat treatment for 24 hours at a peak temperature of 900°C and after 35 hours at a peak temperature of 1200°C are presented in Figs. 29a and 29b, respectively (the silver peaks detected in Fig. 29a were due to the use of a silver specimen holder). The XRD pattern after 900°C treatment show major peaks for hexacelsian, cristobalite, barium mono-aluminate, and silicon nitride. Further treatment at 1200°C yielded additional hexacelsian and a loss of almost all of the mono-aluminate, although a significant amount of cristobalite remained. The cristobalite retained in this specimen may have been produced by the oxidation of some of the silicon nitride during heat treatments at ≤900°C conducted in flowing oxygen. In any event, predominant peaks for monoclinic celsian were not detected in this type of specimen after

III. Results and Discussion (cont.)

A. Synthesis of Celsian Composites (cont.)

3. Silicon Nitride-bearing Composites

b) Reaction Products (cont.)

prolonged annealing at 1200°C. While the preliminary data in Fig. 29 indicates that a significant amount of the compound $BaAl_2Si_2O_8$ can be produced at 1200°C in flowing nitrogen while retaining Si_3N_4, additional work (perhaps involving partial strontium substitution for barium) is needed to evaluate processing conditions leading to monoclinic celsian/silicon nitride composites.

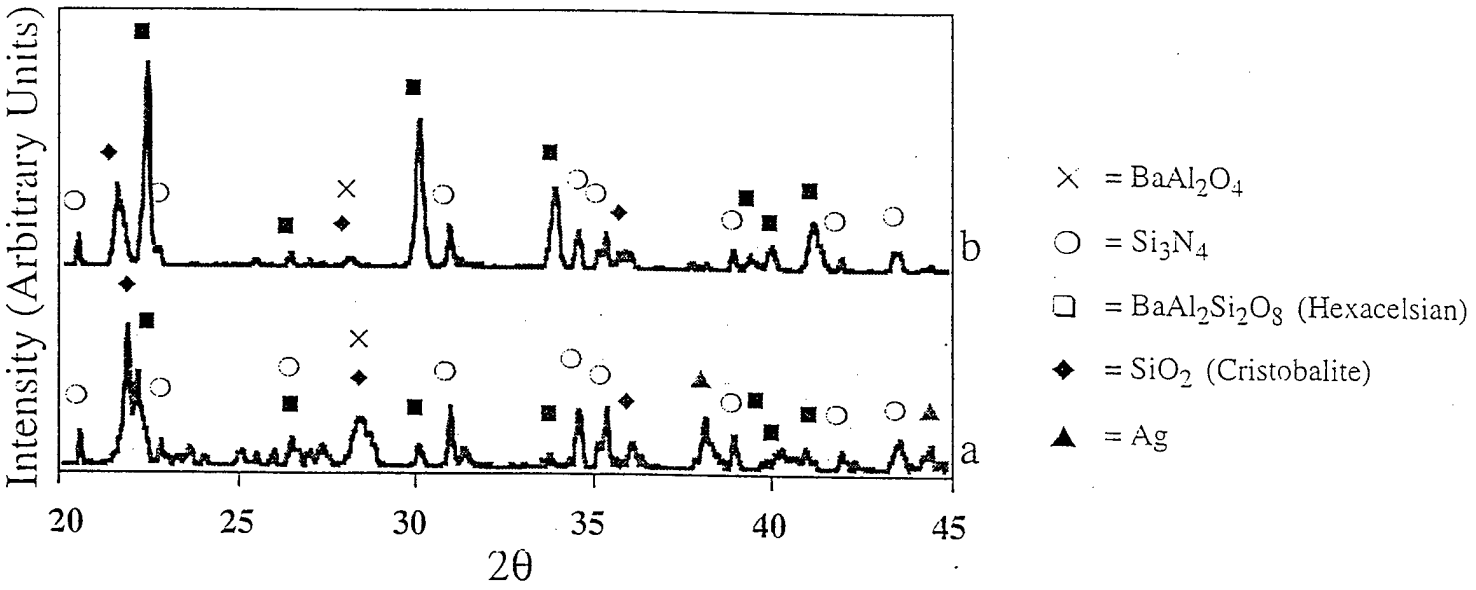

Figure 29b. XRD diffraction patterns of powderized Ba-Al-Al_2O_3-SiO_2-Si_3N_4 specimens after exposure (a) in flowing oxygen at a peak temperature of 900°C for 24 hours, and (b) in flowing nitrogen at a peak temperature of 1200°C for 35 hours.

IV. Conclusions

Two goals of this one-year program were of an applied research nature: 1) to demonstrate that near net-shaped celsian bodies could be produced, and 2) to demonstrate that celsian-matrix composites could be fabricated by the SMP method. A more fundamental research aim was to develop a better understanding of phase/microstructural evolution during the transformation of metallic and metal-oxide precursors into celsian. These applied and basic research goals have been achieved.

Malleable, alkaline-earth-bearing precursors have been fabricated by rolling or pressing of mechanically-alloyed metal or metal+oxide powders. Phase-pure monoclinic celsian or celsian-bearing composites were produced upon oxidation and post-oxidation annealing of such all-metallic and metal+oxide precursors. Complete transformation of appropriate Ba-Al-Al_2O_3-SiO_2 and Ba-Sr-Al-Al_2O_3-SiO_2 precursors yielded near net-shaped celsian bodies (i.e., the dimensional changes before and after complete transformation were ≤1%). Composites of celsian with zirconia were successfully fabricated. The amount of free zirconia increased as the firing temperature increased from 1200-1580°C, which suggested that appreciable solid solubility of zirconia in monoclinic celsian was possible at the lower temperature. Dimensional changes before and after complete transformation of Ba-Al_2O_3-Si-SiO_2-ZrO_2 precursor pellets into celsian-zirconia composites were 1-3%, which indicated that celsian-zirconia composites can be

IV. Conclusions (cont.)

produced with a retention of shape by the SMP method. Altex™ (Al_2O_3-rich) fiber-bearing composites were also produced. Appreciable chemical interaction of the oxidized precursor with the fibers at ≤1260°C was not observed. Attempts at producing celsian-silicon nitride composites at ≤1200°C resulted in the formation of a mixture of hexacelsian, and silicon nitride, along with an appreciable amount of silica.

The reaction path to celsian from Ba-Al-Si precursors over the temperature range of 300-1260°C has been evaluated using XRD, SEM/EDX, EPMA, and TEM. Barium oxidation occurred rapidly at 300°C. The resulting BaO_2 reacted primarily with Si at 300-500°C to yield Ba_2SiO_4. High-resolution TEM analyses of interfaces between BaO_2 and Si revealed that this reaction involved the formation of a thin layer of amorphous silicate located between BaO_2 and Ba_2SiO_4. An amorphous phase was also detected at interfaces between BaO_2 and Al, although the extent of reaction was much lower than for BaO_2 and Si at 300-500°C. During heating (1°C/min) between 500 and 800°C, appreciable oxidation of the aluminum particles within the Ba-Al-Si precursor had occurred. Continued oxidation of Si and reaction of the resulting SiO_2 with Al_2O_3 and Ba_2SiO_4 at 800-1100°C resulted in the formation of other binary silicates ($Al_6Si_2O_{13}$, $Ba_2Si_3O_8$) and hexacelsian, $BaAl_2Si_2O_8$. At 1200-1260°C, hexacelsian transformed into monoclinic celsian. The complete transformation to monoclinic celsian occurred within 102 hours at 1200-1260°C, which is a shorter annealing period than has been reported for other types of precursors. TEM analyses revealed the presence of an amorphous silicate, along with crystals of $BaAl_2Si_2O_8$, in specimens quenched from 1200°C. The composition of the amorphous silicate suggested that the hexagonal-to-monoclinic transformation may have been assisted by the presence of a liquid oxide at 1200°C.

The reaction path to celsian from Ba-Al-Al_2O_3-SiO_2 precursors has also been evaluated. As for Ba-Al-Si precursors, extensive Ba_2SiO_4 formation occurred within 24 hours at 300°C. In other words, appreciable formation of Ba_2SiO_4 by the reaction of oxidized barium with a silicon source occurred at ≤300°C whether the silicon source was Si or SiO_2. Unlike Ba-Al-Si precursors, however, extensive formation of crystalline $BaAl_2O_4$ was detected at ≥300°C. The presence of some Al_2O_3 in the precursor appears to have allowed for the formation of some $BaAl_2O_4$ prior to complete consumption of the reactant BaO_2 (by the concurrent reaction of BaO_2 with SiO_2 to form Ba_2SiO_4). Between 650 and 900°C, hexacelsian formation commenced at the expense of barium aluminate, silica, and barium silicate. Appreciable formation of $BaAl_2Si_2O_8$ had occurred after heat treatment for 35 hours at 1200°C, although complete consumption of barium aluminate and barium silicates required heat treatments in excess of 20 hours at 1500°C. As for Ba-Al-Si specimens, hexacelsian preceded the formation of monoclinic celsian at 1200°C. However, substitution of half of the barium with strontium dramatically enhanced the formation of monoclinic celsian formation at ≤1200°C. Partial substitution of Mg for Ba also enhanced the hexacelsian-to-monoclinic celsian transformation, although an appreciable amount of barium osumilite, $BaMg_2Al_6Si_9O_{30}$, was also produced.

V. Future Work

The work conducted in this project has raised a number of fundamental and applied questions that will be explored in an AFOSR project that commenced on June 1, 1995 (contract #F49620-95-1-0372). The goals of this new project are:

- To further explore and better understand the novel, low-temperature reaction paths and associated oxidation and transformation mechanisms leading to the formation of celsian from metal-bearing precursors.
- To determine whether chemically-homogeneous precursors, or precursors containing phases on a finer scale, can be transformed rapidly into celsian at temperatures well below 1100°C.

V. Future Work (cont.)

- To determine the high-temperature creep resistance and fracture toughness of dense, SMP-derived monolithic celsian and celsian-matrix composites.
- To determine whether the SMP method can be applied to other classes of refractory ceramic compounds.

Little work has been conducted at OSU to date to understand how the rate of oxidation of celsian precursors is influenced by SMP processing. In the new AFOSR program, the rate of oxidation of celsian precursors at various temperatures and oxygen partial pressures will be determined by thermogravimetric analysis (TGA). The influence of processing conditions on the oxidation kinetics will be carefully examined. Processing modifications will be aimed at altering: 1) the extent of interconnected porosity in the barium oxide-bearing phases that are produced at low temperatures (by choosing oxidation conditions that lead to either BaO or BaO_2), 2) the sizes of the discrete aluminum and silicon-bearing metal phases, and 3) the amounts of oxide and metal phases (Al vs. Al_2O_3, Si vs. SiO_2) in the starting precursor.

A number of intermediate oxide compounds ($Al_6Si_2O_{13}$, Ba_2SiO_4, $Ba_2Si_3O_8$, $BaSi_2O_5$) have been detected in Ba-Al-Si and Ba-Al-Al_2O_3-SiO_2 precursors annealed between 800 and 1200°C. While it is known that these oxide phases reacted to form hexacelsian above 1100°C, the exact sequence of reactions leading to hexacelsian is not yet clear. The mechanism of transformation from metastable hexacelsian to stable monoclinic celsian is also not known. TEM analyses have revealed the presence of an amorphous oxide phase in samples quenched from a peak temperature of 1200°C (see Fig. 14). If the amorphous oxide had been present as a transient liquid at elevated temperatures, then the transformation of hexacelsian to monoclinic celsian may be occurring by a dissolution/reprecipitation mechanism (i.e., metastable hexacelsian may dissolve into the liquid oxide and stable monoclinic celsian may precipitate out from the liquid). Such a mechanism is responsible for polymorphic transformations of other metastable silicates (e.g., the cristobalite to tridymite transformation in lime-doped, silica-rich refractories [78]) and is consistent with the observed effect of fluxing agents on the rate of transformation of hexacelsian to celsian [23, 56, 61-65, 68]. Further TEM analyses are underway to evaluate whether such a dissolution/reprecipitation mechanism is responsible for monoclinic celsian formation.

The influence of processing conditions on the rate of transformation to celsian will be examined by modifying the SMP process so as to alter the sizes of the discrete aluminum and silicon-bearing phases. If hexacelsian is forming by the solid-state reaction of a number of intermediate oxide phases, and if the rate of transformation to hexacelsian is limited by solid-state diffusion, then a reduction in the sizes of the intermediate oxide phases may result in a faster rate of transformation to hexacelsian (i.e., finer intermediate oxide phases may result in shorter diffusion paths). It may be possible to reduce the sizes of the intermediate oxide phases by starting with much finer phases in the precursor[12]. Alternately, a chemically-homogeneous $BaAl_2Si_2$ compound precursor could be used. In this case, the barium, aluminum, and silicon are atomically mixed. Low-temperature oxidation of such an atomically-mixed precursor may result in a very fine, intimate mixture of intermediate oxide phases that can react quickly or at very low temperatures into hexacelsian. $BaAl_2Si_2$ precursors can be produced by melt processing (see discussion on pages 5 and 6) or possibly by prolonged mechanical alloying of elemental barium, aluminum, and silicon. A mixture of $BaAl_2Si_2$ with ductile metal phases (e.g., Ba, Al) may be sufficiently malleable as to be compacted and formed into a dense, shaped precursor body.

---

[12] The rate of transformation of mechanically-alloyed Ba-Ti precursors to $BaTiO_3$ is strongly influenced by the extent of mechanical alloying of the metallic precursor powder [1, 5]. This may be due to the refinement of barium and titanium phases in the Ba-Ti precursors with prolonged milling, such that the diffusion distances involved in the later stages of transformation to $BaTiO_3$ were reduced.

V. Future Work (cont.)

Work will continue on the use of the SMP method to produce fiber-reinforced celsian-matrix composites. The influence of the fibers on SMP processing (e.g., formability of the fiber-bearing precursors, influence of the fibers on densification kinetics) will be determined. Of particular interest is the influence of SMP processing on the physico-chemical state of the fiber-matrix interface. If dense fiber-reinforced composites can be produced with low sintering temperatures, little chemical reaction should occur between the matrix and the fibers. The absence of strong chemical bonding between the matrix and the fibers may allow for appreciable toughening by a fiber pullout mechanism in the final composites.

While celsian is an attractive refractory material for ceramic matrices, the synthesis of a few other alkaline-earth-bearing aluminosilicate ceramics will also be examined (as time permits). Such compounds include barium osumilite ($BaMg_2Al_6Si_9O_{30}$) and cordierite ($Mg_2Al_4Si_5O_{18}$). These alkaline earth-bearing oxide compounds possess modest thermal expansion coefficients and good thermal shock resistance (relative to other ceramics). Indeed, cordierite is widely used as a low-expansion, thermal-shock-resistant ceramic (e.g., it is used as a substrate for catalytic converters used to reduce undesired emissions in automobiles). Exploratory studies will involve examination of the formability of the metal-bearing precursors to such compounds, the oxidation kinetics of the precursors, and the rate of transformation of the oxidized precursors to the final ceramic phase. Precursor systems that are formable and can be transformed rapidly into the desired ceramic phases will be considered for further development as a ceramic matrix material.

VI. References

1. M. M. Anthony, K. H. Sandhage, "Barium Titanate/Noble Metal Laminates Prepared by the Oxidation of Solid Metallic Precursors," J. Mater. Res. , **8** (1993) 2968-2977
2. K.H. Sandhage, M.M. Anthony, H.J. Schmutzler, "Synthesis of Ferroelectric Ceramics by the Oxidation of Metallic Precursors," Ceram. Trans., **32** (1993) 49-59
3. K. H. Sandhage, "Process for Making Ceramic/Metal and Ceramic/Ceramic Laminates by Oxidation of a Metal Precursor," U.S. Patent #5,259,885, Nov. 9, 1993
4. K. H. Sandhage, "Electroceramics and Process for Making the Same," U.S. Patent #5,318,725, June 7, 1994
5. H. J. Schmutzler, M.M. Anthony, K.H. Sandhage, "A Novel Reaction Path to $BaTiO_3$ by the Oxidation of a Solid Metallic precursor," J. Am. Ceram. Soc., **77** (1994) 721-729
6. G. A. Ward and K. H. Sandhage, The Synthesis of Magnetic Barium Ferrite, $BaO{\cdot}6Fe_2O_3$, by the Oxidation of Solid Metallic Precursors, Paper presented at the Magnetic Ceramics Symposium (Abstract No. SX III-39-94), 96th Annual American Ceramic Society Meeting, Indianapolis, IN, April 27, 1994
7. H. J. Schmutzler, K. H. Sandhage, J. C. Nava, "The Fabrication of Dense, Shaped Barium Cerate by the Oxidation of Solid Metal-Bearing Precursors," in press
8. G.J. Yurek, J. B. Vander Sande, W.-X. Wang, D. A. Rudman, "Direct Synthesis of a Metal/Superconducting Oxide Composite by Oxidation of a Metallic Precursor," J. Electrochem. Soc., **134** (1987) 2635-2636
9. Y. Yamada, S-I. Murasaki, U. Mizutani, "Preparation of High-T_C Ceramic Superconductors Through Oxidation of Mechanically Alloyed Master Alloy Powders," Jpn. J. Appl. Phys., **27** (1988) L802-803
10. W. Gao, S.-C. Li, D. A. Rudman, G. J. Yurek, J. B. Vander Sande, "Oxidation of Bi(Pb)-Sr-Ca-Cu-Ag Metallic Precursors to Produce Oxide/Ag Superconducting Microcomposites," J. Electrochem. Soc., **137** (1990) 1951-1957
11. K.H. Sandhage, W. Carter, L. Masur, C. Joshi, H. Hsu, G. J. Yurek, "Synthesis of a Ba-Pb-Bi-O/Ag Superconducting Composite by the Oxidation of a Ba-Pb-Bi-Ag Metallic Precursor," Physica C, **177** (1991) 95-100

VI. References (cont.)

12. K. H. Sandhage, L. J. Masur, G. D. Smith, J. M. Poole, M. G. McKimpson, "The Metallic Precursor Approach to Long Lengths of $YBa_2Cu_3O_x$ Superconducting Wire," pp. 347-362 of High Temp. Superconducting Compounds III: Processing and Microstructure Property Relationships, Ed. S. H. Whang, A. DasGupta, E. Collings, The Minerals, Metals, and Materials Society, Warrendale, PA, 1991
13. K. H. Sandhage, "The Preparation of Superconducting $YBa_2Cu_3O_{7-y}$/Ag Microlaminates by an Oscillating Oxidation Scheme," J. Electrochem. Soc., **139** (1992) 1662-1671
14. J. S. Luo, N. Merchant, V. A. Maroni, D. M. Gruen, B. S. Tani, K. H. Sandhage, C. A. Craven, "Growth of C-Axis-Oriented Films of $YbBa_2Cu_3O_{7-y}$ on Single and Polycrystalline MgO Substrates by Oxidation of a Liquid Alloy Precursor," Physica C, **192** (1992), 356-361
15. A. Otto, C. Craven, D. Daly, E. R. Podtburg, J. Schreiber, L. J. Masur, "Properties of High-T_c Wires Made by the Metallic Precursor Process," J. Metals, **45** [9] (1993), 48-52
16. S. M. Allameh, K. H. Sandhage, "Synthesis of Alkaline-Earth Aluminosilicate Ceramics and Ceramic Composites by the Oxidation of Solid Metal-Bearing Precursors," Paper presented at the 19th Annual Cocoa Beach Conference on Composites and Advanced Ceramics (Abstract No. SI-18-95F), American Ceramic Society, Cocoa Beach, FL, Jan. 10, 1995
17. K. H. Sandhage, "Processes for Fabricating Structural Ceramic Bodies and Structural Ceramic-Bearing Composite Bodies," U.S. Patent #5,447,291, Sept. 5, 1995
18. H. J. Schmutzler, K. H. Sandhage, "Formation of Shaped Celsian ($BaAl_2Si_2O_8$) Bodies by the Oxidation of Solid Metallic Precursors," pp. 113-124 in Processing and Fabrication of Advanced Materials: Ceramic and Ceramic Matrix Composites, ed. V. A. Ravi, T. S. Srivatsan, and J. J. Moore. The Minerals, Metals, & Materials Society, Pittsburgh, PA, 1994
19. J. S. Moya Corral and A. Gracia Verduch, "The Solid Solution of Silica in Celsian," Trans J. Brit. Ceram. Soc., **77** (1978) 40-44
20. J. V. Smith and W. L. Brown, pp. 24-25 in Feldspar Mineralogy, Vol. 1: Crystal Structure, Physical, Chemical, and Microtextural Properties, Springer Verlag, Berlin, Germany, 1988
21. H. C. Lin and W. R. Foster, "Studies in the System BaO-Al_2O_3-SiO_2: V, The Ternary System Sanbornite-Celsian-Silica," J. Am. Ceram. Soc., **53** (1970) 549-551
22. C. E. Semler, W. R. Foster, "Studies in the System BaO-Al_2O_3-SiO_2:VI, The System Celsian-Silica-Alumina," J. Am. Ceram. Soc., **53** (1970) 595-598
23. J.C. Debsikdar and O.S. Sowemimo, "Effect of Zirconia Addition on Crystallinity, Hardness, and Microstructure of Gel-derived Barium Aluminosilicates, $BaAl_2Si_2O_8$," J. Mater. Sci. , **27** (1992) 5320-5324
24. D. W. Freitag, "In-situ Processed Si_3N_4 Whiskers in the System BAS-Si_3N_4," Paper presented at ONR Workshop on "Novel and In-Situ Processing of Advanced Materials" June 7-9, 1994, Woods Hole, MA.
25. A. Bandyopadhyay, P. B. Aswath, W. D. Porter, O. B. Cavin, "The Low Temperature Hexagonal to Orthorhombic Transformation in Si_3N_4-Reinforced BAS Matrix Composites," J. Mater. Res., **10** (1995) 1256-1263
26. A. Bandyopadhyay, S. W. Quander, P. B. Aswath, D. W. Freitag, K. K. Richardson, D. L. Hunn, "Kinetics of In-Situ α to β Si_3N_4 Transformation in a Barium Aluminosilicate Matrix," Scripta Met. Mat., **32** (1995) 1417-1422
27. J. A. Zaykoski, I. G. Talmy, "Toughening of Celsian ($BaO{\cdot}Al_2O_3{\cdot}2SiO_2$) Ceramics," Proc. 14th Conf. on Metal-Matrix, Carbon, Ceramic-Matrix Composites, NASA Conf. Publ. 3097, Part 1, 1990, 251-263
28. J. A. Zaykoski, I. G. Talmy, A. Mansour, "Toughening of Celsian Ceramics for Radomes," Proc. 16th Conf. on Metal-Matrix, Carbon, Ceramic-Matrix Composites, NASA Conf. Publ. 3175, Part 1, 1992, 237-245
29. A. G. Merzhanov, I. P. Borovinskaya, "Self-Propagating High-Temperature Synthesis of Refractory Inorganic Compounds," Dokl. Akad. Nauk. SSSR, **204** (1972) 429-32
30. Z. A. Munir, "Synthesis of High Temperature Materials by Self-Propagating Combustion Methods," Bull. Am. Ceram. Soc., **67** (1988) 342-349
31. N. Claussen, T. Le, S. Wu, "Low-Shrinkage Reaction-Bonded Alumina," J. Eur. Ceram. Soc., **5** (1989) 29-35

VI. References (cont.)

32. N. Claussen, N. A. Travitzky, S. Wu, "Tailoring of Reaction-Bonded Al_2O_3 (RBAO) Ceramics," Ceram. Eng. Sci. Proc., **11** (1990) 806-20
33. S. Wu, N. Claussen, "Fabrication and Properties of Low-Shrinkage Reaction-Bonded Mullite," J. Am. Ceram. Soc., **74** (1991) 2460-63
34. S. Wu, D. Holz, N. Claussen, "Mechanisms and Kinetics of Reaction-Bonded Aluminum Oxide Ceramics," J. Am. Ceram. Soc., **76** (1993) 970-980
35. M. S. Newkirk, A. W. Urquhart, H. R. Zwicker, E. Breval, "Formation of Lanxide™ Ceramic Composite Materials," J. Mater. Res., **1** (1986) 81-89
36. M. S. Newkirk, H. D. Lesher, D. R. White, C. R. Kennedy, A. W. Urquhart, T. D. Claar, "Preparation of Lanxide™ Ceramic Matrix Composites: Matrix Formation by the Directed Oxidation of Molten Metals," Ceram. Eng. Sci. Proc., **8** (1987) 879-885
37. A. S. Nagelberg, "Observations on the Role of Mg and Si in the Directed Oxidation of Al-Mg-Si Alloys," J. Mater. Res., **7** (1992) 265-268
38. M. C. Breslin, "Process for Preparing Ceramic-Metal Composite Bodies," U.S. Patent #5,214,011, May 25, 1993
39. M. C. Breslin, J. Ringnalda, J. Seeger, A. L. Marasco, G. S. Daehn, H. L. Fraser, "Alumina/Aluminum Co-Continuous Ceramic Composite (C^4) Materials Produced by Solid/Liquid Displacement Reactions: Processing Kinetics and Microstructures," Ceram. Eng. Sci. Proc., **15** (1994) 108-112
40. M. C. Breslin, J. Ringnalda, L. Xu, M. Fuller, J. Seeger, G. S. Daehn, T. Otani, H. L. Fraser, "Processing, Microstructure, and Properties of Co-Continuous Alumina-Aluminum Composites," Mater. Sci. Eng. A, **195** (1995) 113-119
41. I. N. Ganiyev, A. V. Vakhobov, T. D. Dzhurayev, "The Ba-Al-Si Phase Diagram," Russian Met., No. 4 (1978), pp. 183-185
42. H. J. Schmutzler, P. Kumar, K. H. Sandhage, unpublished work conducted at The Ohio State University, 1994-95
43. O. Kubaschewski, B. E. Hopkins, Oxidation of Metals and Alloys, Second Edition, Butterworth, London, 1962, 40, 213-15
44. N. B. Pilling, R. E. Bedworth, "The Oxidation of Metals at High Temperatures," J. Inst. Metals, **29** (1923), 529-82
45. T. E. Leontis, F. N. Rhines, "Rates of High-Temperature Oxidation of Magnesium and Magnesium Alloys," Trans. A.I.M.E., **166** (1946), 265-94
46. W. M. Fassell, L. B. Gulbransen, J. R. Lewis, J. H. Hamilton, "Ignition Temperature of Magnesium and Magnesium Alloys," J. Metals, **171** (1951), 522-28
47. D. Cubicciotti, "The Oxidation of Calcium at Elevated Temperatures," J. Am. Chem. Soc., **74** (1952), 557-58
48. M. S. Chandrasekharaiah, J. L. Margrave, "The Kinetics of Oxidation and Nitridation of Lithium, Calcium, Strontium, and Barium," J. Electrochem. Soc., **108** (1961), 1008-1012
49. R. Streiff, "Study of Calcium Oxidation: Reaction Mechanisms," Acta Met., **16** (1968), 1227-38
50. R. Citak, H. J. Schmutzler, K. H. Sandhage, unpublished work conducted at Ohio State University, 1994
51. G. Bruzzone, M. Ferretti, F. Merlo, "The Ba-Ag System," J. Less-Common Met., **128** (1987), 259-264
52. Constitution of Binary Alloys, M. Hansen (ed.), Genium Publishing Co., Schenectady, NY, 1991, pg. 37
53. I. Barin, Thermochemical Data of Pure Substances, VCH Verlagsgesellschaft, Weinheim, Germany, 1989, vols. 1-2
54. O. Knacke, O. Kubaschewski, K. Hesselmann, Thermochemical Properties of Inorganic Substances, 2nd Edition, Springer-Verlag, Berlin, 1991, vols. 1-2.
55. J.E.Planz and H. Müller-Hesse, "Untersuchungen uber Festkorperreaktionen im System BaO-Al_2O_3-SiO_2 Teil II: Uber die Celsianbildung durch Festkorperreactionen," Ber. Dtsch. Keram. Ges., **40** (1963) 191-200
56. N. P. Bansal and M. J. Hyatt, "Crystallization Kinetics of BaO-Al_2O_3-SiO_2 Glasses," J. Mater. Res., **4** (1989) 1257-1265

VI. References (cont.)

57. J. S. Moya. Corral and A.G. Verduch, "Estudio de la Reaccion Entre el Caloin y el Carbonato de Bario," Bol. Soc. Esp. Ceram. Vidr., **15** (1976) 379-381
58. M.C. Guillem and C. Guillem, "Kinetics and Mechanism of Formation of Celsian from Barium Carbonate and Kaolin," Br. Ceram. Trans. J., **83** (1984) 150-154
59. C.A. Sorrell, "Solid State Formation of Barium, Strontium and Lead Feldspars in Clay-Sulfate Mixtures," Am. Miner., **47** (1962) 291-309
60. W. K. Treadway, S.H. Risbud, "Gel Synthesis of Glass Powders in the $BaO{\cdot}Al_2O_3{\cdot}2SiO_2$ System," J. Non-Cryst. Solids, **100** (1988) 278-283
61. M. Chen, W.E. Lee, and P.F. James, "Preparation and Characterization of Alkoxide-Derived Celsian Glass-Ceramic," J. Non-Cryst. Solids, **130** (1991) 322-325
62. J.C. Debsikdar, "Gel to Glass Conversion and Crystallization of Alkoxy-derived Barium Aluminosilicate Gel," J. Non-Cryst. Solids, **144** (1992) 269-276
63. M. Chen, W. E. Lee, P. F. James, "Synthesis of Monoclinic Celsian Glass-Ceramic from Alkoxides," J. Non-Cryst. Solids, **147&148** (1992) 532-536
64. A. D. Cozzi, Z. Fathi, D. E. Clark, "Crystallization of Sol-Gel Derived Barium Aluminosilicate in a 2.45 GHz Microwave Field," Ceram. Trans., **36** (1992) 318-324
65. J. C. Debsikdar, "Sol-Gel Route to Celsian Ceramic," Ceram. Eng. Sci. Proc., **14** (1993) 405-415
66. D. Bahat, "Heterogeneous Nucleation of Alkaline Earth Feldspar Glasses, " J. Mater. Sci., **4** (1969) 847-854
67. D. Bahat, "Kinetic Study of the Hexacelsian-Celsian Phase Transformation," J. Mater. Sci., **5** (1970) 805-810
68. C. H. Drummond, III, W. E. Lee, N. P. Bansal, M. J. Hyatt, "Crystallization of Barium Aluminosilicate Glass," Ceram. Eng. Sci. Proc., **10** (1989) 1485-1502
69. I. G. Talmy, D. A. Haught and E. J. Wuchina, "Ceramics in the System $BaO{\cdot}Al_2O_3{\cdot}2SiO_2$-$SrO{\cdot}Al_2O_3{\cdot}2SiO_2$ (BAS-SAS): Polymorphism, Processing, and Properties," pp. 687-698 in Proc. 6th Int. SAMPE Electronics Conf., Vol. 6, Critical Materials and Processing in a Changing World. Ed. A. B. Goldberg, C. A. Harper, M. S. Schroeder, A. M. Ibrahim, SAMPE, Baltimore, MD, 1992
70. J. A. Zaykoski, I. G. Talmy, "Gallium and Germanium Substitutions in Celsian," Ceram. Eng. Sci. Proc., **15** (1994) 779-786
71. N. A. Sirazhiddinov, P. A. Arifov, R. G. Grebenshchikov "Isomorphism in the System $SrAl_2Si_2O_8$-$BaAl_2Si_2O_8$," Izv. Akad. Nauk SSSR, Neorg. Mater., **8**, (1972) 870-874
72. N. P. Bansal, M. J. Hyatt, "Crystallization and Properties of Sr-Ba Aluminosilicate Glass-Ceramic Matrices," Ceram. Eng. Sci. Proc., **12** (1991) 1222-1234
73. F. F. Lange, "Transformation Toughening, Part 4, Fabrication, Fracture, Toughness, and Strength of Al_2O_3-ZrO_2 Composites," J. Mater. Sci., **17** (1982), 247-254
74. K. Tsukuma, K. Ueda, "Strength and Fracture Toughness of Isostatically Hot-Pressed Composites of Al_2O_3 and Y_2O_3-partially-stabilized ZrO_2," J. Am. Ceram. Soc., **68** (1985), C-4 - C-5
75. Y. Matsumoto, K. Hirota, O. Yamaguchi, S. Inamura, H. Miyamoto, N. Shiokawa, K. Tsuji, "Mechanical Properties of Hot Isostatically Pressed Zirconia-Toughened Alumina Prepared from Coprecipitated Powders," J. Am. Ceram. Soc., **76** (1993), 2677-80
76. N. Claussen, J. Jahn, "Mechanical Properties of Sintered, In Situ-Reacted Mullite-Zirconia Composites," J. Am. Ceram. Soc., **63** (1980), 228-229
77. Q. M. Yuan, J. Q. Tan, Z. G. Jin, "Preparation and Properties of Zirconia-Toughened Mullite Ceramics," J. Am. Ceram. Soc., **69** (1986), 265-67
78. W. D. Kingery, H. K. Bowen, D. R. Uhlmann, Introduction to Ceramics, 2nd Edition, John Wiley & Sons, New York, 1976, pg. 543

VII. Publications/Presentations

Work from this project has been, or will be, published or presented as follows:

1) H. J. Schmutzler, K. H. Sandhage, "Transformation of Ba-Al-Si Precursors to Celsian by High-Temperature Oxidation and Annealing," Met. Mat. Trans., **26B** (1995), pp. 135-148

2) S. M. Allameh, K. H. Sandhage, "Synthesis of Alkaline-Earth Aluminosilicate Ceramics and Ceramic Composites by the Oxidation of Solid Metal-Bearing Precursors," Paper presented at the 19th Annual Cocoa Beach Conference on Composites and Advanced Ceramics (Abstract No. SI-18-95F), American Ceramic Society, Cocoa Beach, FL, Jan. 10, 1995

3) S. M. Allameh, K. H. Sandhage, H. L. Fraser, "A Solid Metal-Bearing Precursor Route for Fabricating Alkaline-Earth-Bearing Aluminosilicate Ceramics and Ceramic-Matrix Composites," Paper presented at the Fall Meeting of the Basic Science Division of the American Ceramic Society (Abstract #B-21-94F), Sept. 26, 1994, Louisville, KY

4) S. M. Allameh, K. H. Sandhage, H. L. Fraser, "A Solid Metal-Bearing Precursor (SMP) Route to Dense, Shaped Alkaline-Earth-Bearing Aluminosilicate Ceramics," Paper presented at the 97th Annual Meeting of the American Ceramic Society (Abstract #SXIX-72-95), May 3, 1995, Cincinnati, OH

5) S. M. Allameh, K. H. Sandhage, H. L. Fraser, "The Fabrication of Shaped Celsian-Bearing Composites by the Oxidation of Solid Metal-Bearing Precursors," Paper presented at the Annual Meeting of the American Ceramic Society (Abstract #C-13-95), May 2, 1995, Cincinnati, OH

6) K. H. Sandhage, S. M. Allameh, H. L. Fraser, "A Novel Solid Metal-Bearing Precursor (SMP) Route to Near Net-Shaped Alkaline-Earth Aluminosilicates," submitted for publication in the Proceedings of the European Ceramic Society Fourth Conference, Oct. 3, 1995, Riccione, Italy

7) S. M. Allameh, K. H. Sandhage, H. L. Fraser, "Synthesis of Near Net-Shaped, Celsian-Bearing Ceramics by the Oxidation of Solid, Metal-Bearing Precursors (SMP)," submitted for publication in the Proceedings of the International Symposium on Processing and Fabrication of Advanced Materials, TMS/ASM, Nov. 2, 1995, Cleveland, OH

Several papers on the phase and microstructural evolution to celsian from metal/oxide precursors, the synthesis of near net-shaped monolithic celsian, and the fabrication of celsian composites are currently being written for publication in peer-reviewed journals.

VIII. Acknowledgements

The results of this final report were largely a consequence of the efforts of the following research scientists:

Dr. Hans J. Schmutzler:	processing and XRD/EPMA characterization of all-metallic precursors
Dr. Seyed M. Allameh:	processing and XRD/EPMA characterization of metal-oxide precursors
Dr. Robert Wheeler:	TEM characterization of all-metallic precursors

Drs. Allameh and Wheeler are continuing work in this area at OSU. Dr. Schmutzler is now at the Commission of the European Communities Joint Research Center (Ispra, Italy).

The financial support of the Air Force Office of Scientific Research is gratefully acknowledged.